Deliyannis, Theodore L. et al "Single Operational Transconductance Amplifier (OTA) Filters"
Continuous-Time Active Filter Design
Boca Raton: CRC Press LLC,1999

Chapter 8

Single Operational Transconductance Amplifier (OTA) Filters

8.1 Introduction

In the previous chapters active RC filters using the operational amplifier (opamp) have been discussed extensively. These filters have been widely used in various low frequency applications in telecommunication networks, signal processing circuits, communication systems, control, and instrumentation systems for a long time. However, active RC filters cannot work at higher frequencies (over 200kHz) due to opamp frequency limitations and are not suitable for full integration. They are also not electronically tunable and usually have complex structures. Many attempts have been made to overcome these drawbacks [1]–[8]. The most successful approach is to use the operational transconductance amplifier (OTA) to replace the conventional opamp in active RC filters [9]–[45], as predicted in [9]. In recent years OTA-based high frequency integrated circuits, filters and systems have been widely investigated.

As seen in Chapter 3, an ideal operational transconductance amplifier is a voltage-controlled current source, with infinite input and output impedances and constant transconductance. The OTA has two attractive features: its tranconductance can be controlled by changing the external dc bias current or voltage, and it can work at high frequencies. The OTA has been implemented widely in CMOS and bipolar and also in BiCMOS and GaAs technologies. The typical values of transconductances are in the range of tens to hundreds of μS in CMOS and up to mS in bipolar technology. The CMOS OTA, for example, can work typically in the frequency range of 50 MHz to several 100 MHz. Linearization techniques make the OTA able to handle input signals of the order of volts with nonlinearities of a fraction of one percent. We will not discuss the OTA design in this book, although it is very important. The reader can look at References [2]–[5] on this topic.

Programmable high-frequency active filters can therefore be achieved by incorporating the OTA. These OTA filters also have simple structures and low sensitivity. In Chapter 3 the OTA and some simple OTA-based building blocks were introduced. In this chapter we will discuss how to construct filters using a single OTA, because single OTA active filters have advantages such as low power consumption, noise, parasitic effects, and cost. Commercially widely available OTAs are very easy to access for one to build filters with resistors and capacitors.

However, single OTA filters may not be suitable for full integration as they contain resistors which demand large chip area. These filter structures may also not be fully programmable, as only one OTA is utilized. It should be emphasized that on-chip tuning is the most effective way to overcome fabrication tolerances, component nonidealities, aging, and changing operating conditions such as temperature. Therefore, in monolithic design we should also further avoid using resistors. In recent years, active filters which use only OTAs and capacitors have been widely studied [12]–[23], [26]–[43]. These filters are intuitively called OTA-C filters, which will also be the subject of the remaining

chapters. Fortunately, the single OTA filter structures can be readily converted into fully integrated OTA-C counterparts by using OTAs to simulate the resistors. This will be shown in the chapter.

It should be noted that practical OTAs will have finite input and output impedances. For the CMOS OTA, for example, the input resistance is usually very large, being neglectable, but the output resistance is in the range of $50k\Omega$ to $1M\Omega$, and the input and output capacitances are typically of the order of $0.05pF$ [7]. Also, at very high frequencies, the OTA transconductance will be frequency dependent due to its limited bandwidth. These nonideal impedance and transconductance characteristics will influence the stability and frequency performances of OTA filters. Practical OTAs will also exhibit nonlinearity for large signals and have noise, which will affect the dynamic range of OTA filters.

In this chapter a large number of first-order and second-order single OTA filter structures are generated systematically. Design methods and equations are derived. Sensitivity analysis is conducted, and OTA nonideality effects are investigated. Performances of the generated OTA filter architectures are also compared. Knowledge of the OTA in Chapter 3 and single opamp active RC filters in Chapter 4 should be of help in understanding this chapter.

8.2 Single OTA Filters Derived from Three-Admittance Model

Consider the general circuit model in Fig. 8.1. It contains one OTA and three admittances. With the indicated input and output voltages it can be simply shown that

$$H_1(s) = \frac{V_{o1}}{V_i} = \frac{g_m Y_2}{Y_1Y_2 + Y_1Y_3 + Y_2Y_3 + g_m Y_2} \tag{8.1}$$

$$H_2(s) = \frac{V_{o2}}{V_i} = \frac{g_m\,(Y_1 + Y_2)}{Y_1Y_2 + Y_1Y_3 + Y_2Y_3 + g_m Y_2} \tag{8.2}$$

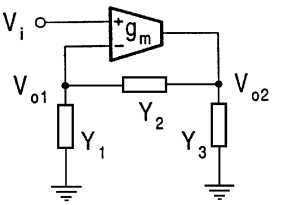

FIGURE 8.1
General model with three admittances.

Using these expressions we can readily derive different first-order and second-order filter structures from the general three-admittance model in Fig. 8.1 by assigning different components to Y_i and checking the corresponding transfer functions in Eqs. (8.1) and (8.2). For example, Y_i can be a resistor ($Y_i = g_i$), a capacitor ($Y_i = sC_i$), an open circuit ($Y_i = 0$), or a short circuit ($Y_i = \infty$). It can also be a parallel combination of two components ($Y_i = g_i + sC_i$).

8.2.1 First-Order Filter Structures

In this section we use the general model to generate first-order filters.

First-Order Filters with One or Two Passive Components

Selecting $Y_1 = sC_1$, $Y_2 = \infty$ and $Y_3 = 0$ gives rise to the simplest structure as shown in Fig. 8.2(a), which has a lowpass filter function given by

$$H_1(s) = \frac{g_m}{sC_1 + g_m} \tag{8.3}$$

with the dc gain equal to unity and the cutoff frequency equal to g_m/C_1.

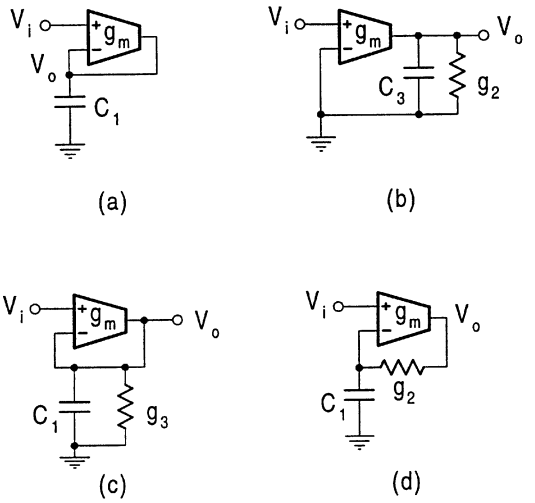

FIGURE 8.2
Simple first-order lowpass (a, b, c) and general (d) filters.

Figure 8.2(b) shows another simple lowpass filter corresponding to $Y_1 = \infty$, $Y_2 = g_2$, and $Y_3 = sC_3$. The transfer function is derived as

$$H_2(s) = \frac{g_m}{sC_3 + g_2} \tag{8.4}$$

with the dc gain equal to g_m/g_2 and the cutoff frequency being g_2/C_3.

The circuit in Fig. 8.2(c), corresponding to $Y_1 = sC_1$, $Y_2 = \infty$ and $Y_3 = g_3$, has the lowpass characteristic as

$$H_1(s) = \frac{g_m}{sC_1 + (g_3 + g_m)} \tag{8.5}$$

When $Y_1 = sC_1$, $Y_2 = g_2$, and $Y_3 = 0$, the output from V_{o2} is a general type, given by

$$H_2(s) = \frac{sg_mC_1 + g_mg_2}{sg_2C_1 + g_mg_2} \tag{8.6}$$

which has the standard form of

$$H(s) = K\frac{s + \omega_z}{s + \omega_p} \tag{8.7}$$

The circuit is shown in Fig. 8.2(d). The circuits in Fig. 8.2 were also discussed, for example, in Ref. [15], here we show that they can be derived from the model in Fig. 8.1.

First-Order Filters with Three Passive Components

Observe that all the circuits in Fig. 8.2 contain less than three passive elements. In Fig. 8.3 we present a set of first-order filters with three passive components, which are derived from Fig. 8.1.

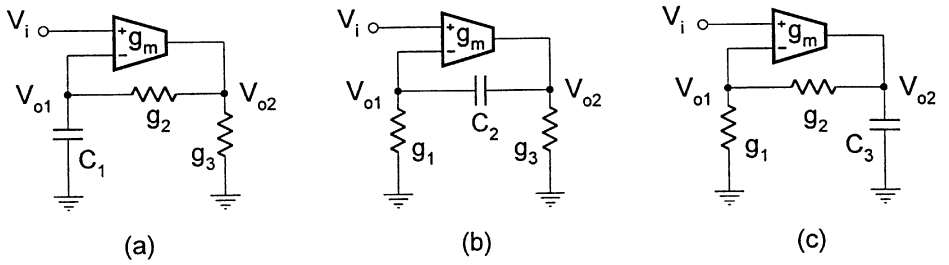

FIGURE 8.3
First-order filter configurations with three passive components.

It is first verified that when choosing $Y_1 = sC_1$, $Y_2 = g_2$ and $Y_3 = g_3$, the general model produces a lowpass filter from V_{o1}, that is

$$H_1(s) = \frac{g_m g_2}{s\,(g_2 + g_3)\,C_1 + g_2\,(g_3 + g_m)} \tag{8.8}$$

and a general transfer function from V_{o2}, given by

$$H_2(s) = \frac{sg_m C_1 + g_m g_2}{s\,(g_2 + g_3)\,C_1 + g_2\,(g_3 + g_m)} \tag{8.9}$$

The circuit is shown in Fig. 8.3(a).

Then consider the circuit in Fig. 8.3(b), which is obtained by setting $Y_1 = g_1$, $Y_2 = sC_2$ and $Y_3 = g_3$. It is found that a highpass filter is derived whose transfer function is given by

$$H_1(s) = \frac{sg_m C_2}{s\,(g_1 + g_3 + g_m)\,C_2 + g_1 g_3} \tag{8.10}$$

with the gain at the infinite frequency being $g_m/(g_1 + g_3 + g_m)$ and the cutoff frequency equal to $g_1 g_3/[(g_1 + g_3 + g_m)C_2]$.

This circuit also offers a general first-order characteristic, as can be seen from its transfer function

$$H_2(s) = \frac{sg_m C_2 + g_m g_1}{s\,(g_1 + g_3 + g_m)\,C_2 + g_1 g_3} \tag{8.11}$$

Finally, if Y_1 and Y_2 are resistors and Y_3 a capacitor, then both $H_1(s)$ and $H_2(s)$ are of lowpass characteristic. The circuit is presented in Fig. 8.3(c) and the transfer functions are given below.

$$H_1(s) = \frac{g_m g_2}{s\,(g_1 + g_2)\,C_3 + g_2\,(g_1 + g_m)} \tag{8.12}$$

$$H_2(s) = \frac{g_m\,(g_1 + g_2)}{s\,(g_1 + g_2)\,C_3 + g_2\,(g_1 + g_m)} \tag{8.13}$$

It is interesting to note from Eqs. (8.8) and (8.12) that the filters in Figs. 8.3(a) and (c) have similar characteristics from output V_{o1} or $H_1(s)$. The circuits in Figs. 8.2(a–c) and 8.3(c) will also be used as lossy integrators to construct integrator-based OTA-C filters in Chapter 9.

8.2.2 Lowpass Second-Order Filter with Three Passive Components

It should be pointed out that the model in Fig. 8.1 can also support many second-order filters. In this section however we only derive and discuss the simplest lowpass filter in order for the reader to appreciate some advantages of OTA filters before a comprehensive investigation of structure generation, design, and performance analysis of various second-order filters using a single OTA. Choosing in Fig. 8.1 $Y_1 = sC_1$, $Y_2 = g_2$, $Y_3 = sC_3$, the transfer function in Eq. (8.1) becomes

$$H_1(s) = \frac{g_m g_2}{s^2 C_1 C_3 + s g_2 (C_1 + C_3) + g_m g_2} \tag{8.14}$$

which is a lowpass filter characteristic. The corresponding circuit is shown in Fig. 8.4, which has only one resistor and two capacitors.

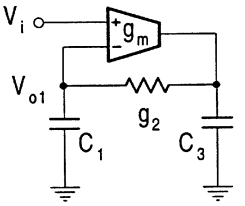

FIGURE 8.4
Simplest second-order lowpass filter derived from Fig. 8.1.

It will be recalled from Chapter 4 that the standard form of the lowpass characteristic is normally written as

$$H_d(s) = \frac{K\omega_o^2}{s^2 + \frac{\omega_o}{Q}s + \omega_o^2} \tag{8.15}$$

where K is the dc gain, ω_o is the undamped natural frequency, and Q is the quality factor, representing the selectivity, that is, the initial steepness of the transition band.

Comparison of Eqs. (8.14) and (8.15) indicates that the dc gain of the filter, K, is unity and

$$\omega_o = \sqrt{\frac{g_m g_2}{C_1 C_3}}, \quad Q = \sqrt{\frac{g_m}{g_2}} \frac{\sqrt{C_1 C_3}}{C_1 + C_3} \tag{8.16}$$

For convenience of design and also from the viewpoint of cost we set $C_1 = C_3$. This permits the development of simple design formulas for the component values, given by

$$C_1 = C_3 = C, \quad g_2 = \frac{\omega_o C}{2Q}, \quad g_m = 2Q\omega_o C \tag{8.17}$$

where C can be arbitrarily assigned.

As an example, we design the filter for the specifications of

$$f_o = 4MHz, \quad Q = 1/\sqrt{2}, \quad K = 1$$

This is a Butterworth filter. Choosing $C_1 = C_3 = C = 5pF$, using Eq. (8.17) we can compute $g_2 = 88.86\mu S$ and $g_m = 177.72\mu S$.

Now we consider the filter sensitivity performance. Using the relative sensitivity definition introduced in Chapter 4, namely,

$$S_x^Q = \frac{x}{Q}\frac{\partial Q}{\partial x}, \quad S_x^{\omega_o} = \frac{x}{\omega_o}\frac{\partial \omega_o}{\partial x} \tag{8.18}$$

for the lowpass filter in Fig. 8.4 it is found that:

$$S_{g_m}^{\omega_o} = S_{g_2}^{\omega_o} = -S_{C_1}^{\omega_o} = -S_{C_3}^{\omega_o} = \tfrac{1}{2} \tag{8.19}$$

$$S_{g_m}^{Q} = -S_{g_2}^{Q} = \tfrac{1}{2}, \quad -S_{C_1}^{Q} = S_{C_3}^{Q} = \tfrac{1}{2}\tfrac{C_1 - C_3}{C_1 + C_3} = 0 \tag{8.20}$$

and these results indicate superior sensitivity performance. Note that setting $C_1 = C_3$ leads not only to practical convenience, but also to a decrease in the sensitivity of the filter to deviations in the capacitor design values, as can be seen from Eq. (8.20).

It is therefore clear from the above discussion that the OTA lowpass filter has a very simple structure, minimum component count, very simple design formulas, and extremely low sensitivity. As will be seen, this is generally true for other OTA filters.

8.2.3 Lowpass Second-Order Filters with Four Passive Components

It is quite straightforward to treat each admittance in the general model as a single passive component, either a resistor or capacitor as seen above. If more components are used for a single admittance, then more filter architectures can be obtained. In the following we generate useful lowpass second-order filters with four passive components, using again the model in Fig. 8.1.

The lowpass filter with $Y_1 = sC_1$, $Y_2 = g_2$, $Y_3 = g_3 + sC_3$ is depicted in Fig. 8.5(a). Its transfer function is derived as

$$H_1(s) = \frac{g_m g_2}{s^2 C_1 C_3 + s\left[(g_2 + g_3)C_1 + g_2 C_3\right] + g_2(g_m + g_3)} \tag{8.21}$$

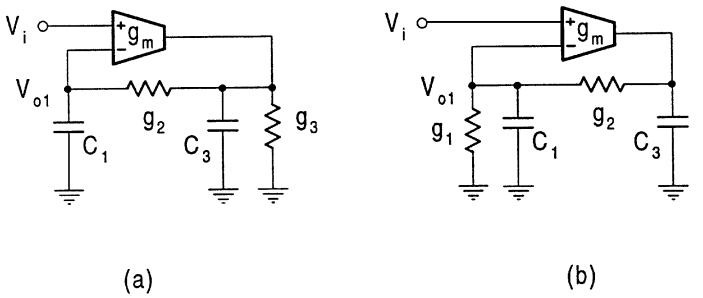

FIGURE 8.5
Lowpass filters with four passive components.

Comparing the transfer function in Eq. (8.21) with the desired function in Eq. (8.15) yields the following equations

$$\omega_o = \sqrt{\frac{g_2(g_3+g_m)}{C_1C_3}}, \quad Q = \frac{\sqrt{g_2(g_3+g_m)C_1C_3}}{(g_2+g_3)C_1+g_2C_3},$$

$$K = \frac{g_m}{g_3+g_m} \tag{8.22}$$

A convenient design is to select $C_1 = C_3 = C$ and $g_2 = g_3 = g$. That is, all capacitances are equal and all conductances are identical, which makes the design easy and economical. With this selection, only three component values need to be decided. Generally, we can determine the component values for given ω_o, Q and K. We can also assign a value to any of C, g, or g_m and determine the other two in terms of ω_o and Q for a not specified K.

For the equal capacitances and conductances Eqs. (8.22) accordingly become

$$\omega_o C = \sqrt{g\,(g+g_m)}, \quad Q = \frac{\sqrt{g(g+g_m)}}{3g}, \quad K = \frac{g_m}{g+g_m} \tag{8.23}$$

From Eqs. (8.23) it can be determined that

$$g = \frac{\omega_o C}{3Q}, \quad g_m = 3Q\omega_o C\left(1 - \frac{1}{9Q^2}\right), \quad K = 1 - \frac{1}{9Q^2} \tag{8.24}$$

It is very interesting to note, see Eqs. (8.24), that

$$Q = \frac{1}{3}, \quad K = 0, \quad g_m = 0 \tag{8.25}$$

$$Q > \frac{1}{3}, \quad K > 0, \quad g_m > 0 \tag{8.26}$$

$$Q < \frac{1}{3}, \quad K < 0, \quad g_m < 0 \tag{8.27}$$

Equation (8.26) indicates that the circuit can realize large Q and positive gain, while Eq. (8.27) implies that with the interchange of the OTA input terminals the resulting circuit will complementarily implement small Q and negative gain. Equation (8.25) means that the design method cannot implement $Q = 1/3$. However, this does not represent a problem, since Q of 1/2 or lower can be realized straightforwardly with a passive RC circuit. We should stress that throughout the chapter, for $g_m > 0$, the OTA is connected just as it appears in figures, while $g_m < 0$ simply means the interchange of the OTA input terminals.

Using the sensitivity definition in Eq. (8.18) it can be derived from Eqs. (8.22) that the general sensitivity expressions are given by

$$S_{C_1}^{\omega_o} = S_{C_3}^{\omega_o} = -S_{g_2}^{\omega_o} = -\frac{1}{2}, \quad S_{g_3}^{\omega_o} = \frac{1}{2}\frac{g_3}{g_3+g_m},$$

$$S_{g_m}^{\omega_o} = \frac{1}{2}\frac{g_m}{g_3+g_m} \tag{8.28}$$

$$S_{C_1}^{Q} = \frac{1}{2} - \frac{(g_2+g_3)\,C_1}{(g_2+g_3)\,C_1 + g_2C_3},$$

$$S_{C_3}^{Q} = \frac{1}{2} - \frac{g_2 C_3}{g_2 C_3 + (g_2 + g_3) C_1},$$

$$S_{g_2}^{Q} = \frac{1}{2} - \frac{g_2 (C_1 + C_3)}{g_2 (C_1 + C_3) + g_3 C_1},$$

$$S_{g_3}^{Q} = \frac{g_3}{2 (g_3 + g_m)} - \frac{g_3 C_1}{g_3 C_1 + g_2 (C_1 + C_3)},$$

$$S_{g_m}^{Q} = S_{g_m}^{\omega_o} \tag{8.29}$$

$$S_{C_1}^{K} = S_{C_3}^{K} = S_{g_2}^{K} = 0, \quad -S_{g_3}^{K} = S_{g_m}^{K} = \frac{g_3}{g_3 + g_m} \tag{8.30}$$

For the design with $C_1 = C_3 = C$ and $g_2 = g_3 = g$, substituting the design formulas in Eqs. (8.24) we have further

$$S_{C_1}^{\omega_o} = S_{C_3}^{\omega_o} = -S_{g_2}^{\omega_o} = -\frac{1}{2}, \quad S_{g_3}^{\omega_o} = \frac{1}{18Q^2},$$

$$S_{g_m}^{\omega_o} = \frac{1}{2}\left(1 - \frac{1}{9Q^2}\right) \tag{8.31}$$

$$S_{C_1}^{Q} = -S_{C_3}^{Q} = S_{g_2}^{Q} = -\frac{1}{6}, \quad S_{g_3}^{Q} = -\frac{1}{3} + \frac{1}{18Q^2},$$

$$S_{g_m}^{Q} = S_{g_m}^{\omega_o} \tag{8.32}$$

$$S_{C_1}^{K} = S_{C_3}^{K} = S_{g_2}^{K} = 0, \quad -S_{g_3}^{K} = S_{g_m}^{K} = \frac{1}{9Q^2} \tag{8.33}$$

It can be seen from these results that the structure in Fig. 8.5(a) has very low sensitivity.

Another lowpass filter can be obtained, which corresponds to $Y_1 = g_1 + sC_1$, $Y_2 = g_2$, $Y_3 = sC_3$, as shown in Fig. 8.5(b). It has the transfer function

$$H_1(s) = \frac{g_m g_2}{s^2 C_1 C_3 + s\left[g_2 C_1 + (g_1 + g_2) C_3\right] + g_2 (g_m + g_1)} \tag{8.34}$$

This lowpass filter is similar to the one discussed above, as can be seen from Eqs. (8.21) and (8.34). The same design technique can be used, and the sensitivity performance is also similar.

8.2.4 Bandpass Second-Order Filters with Four Passive Components

The bandpass filter with $Y_1 = g_1$, $Y_2 = sC_2$, $Y_3 = g_3 + sC_3$ is shown in Fig. 8.6(a). The circuit transfer function is derived as

$$H_1(s) = \frac{s g_m C_2}{s^2 C_2 C_3 + s\left[(g_1 + g_3 + g_m) C_2 + g_1 C_3\right] + g_1 g_3} \tag{8.35}$$

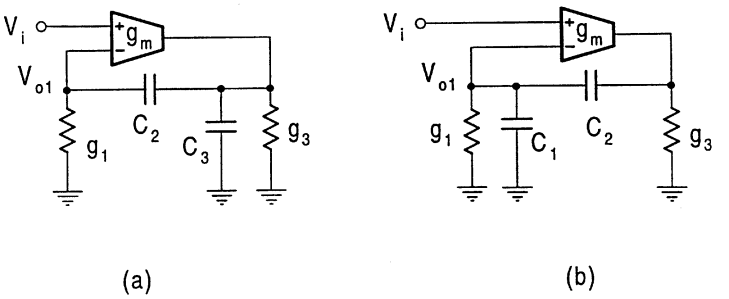

FIGURE 8.6
Bandpass filters with four passive components.

The ideal bandpass characteristic is typically written as

$$H_d(s) = \frac{K\frac{\omega_o}{Q}s}{s^2 + \frac{\omega_o}{Q}s + \omega_o^2} \tag{8.36}$$

where ω_o is the geometric center frequency of the passband, ω_o/Q is the $3dB$ bandwidth, which can also be denoted by B, and Q is again the quality factor.

Comparing Eq. (8.35) with Eq. (8.36) leads to the following design equations:

$$\omega_o = \sqrt{\frac{g_1 g_3}{C_2 C_3}}, \quad Q = \frac{\sqrt{g_1 g_3 C_2 C_3}}{(g_1 + g_3 + g_m)\,C_2 + g_1 C_3},$$

$$K = \frac{g_m C_2}{(g_1 + g_3 + g_m)\,C_2 + g_1 C_3} \tag{8.37}$$

We set $C_2 = C_3 = C$ and $g_1 = g_3 = g$ and obtain from Eqs. (8.37)

$$g = \omega_o C, \quad g_m = \frac{\omega_o C}{Q}(1 - 3Q), \quad K = 1 - 3Q \tag{8.38}$$

It can be seen from Eq. (8.38) that for practical Q values, $g_m < 0$ and $K < 0$ which mean that the OTA input terminals need to be interchanged and negative gain will be achieved.

The sensitivities of the filter are found to be

$$S_{C_2}^{\omega_o} = S_{C_3}^{\omega_o} = -S_{g_1}^{\omega_o} = -S_{g_3}^{\omega_o} = -\frac{1}{2}, \quad S_{g_m}^{\omega_o} = 0 \tag{8.39}$$

$$-S_{C_2}^{Q} = S_{C_3}^{Q} = \frac{1}{2} - \frac{g_1 C_3}{g_1 C_3 + (g_1 + g_3 + g_m)\,C_2},$$

$$S_{g_1}^{Q} = \frac{1}{2} - \frac{g_1 (C_2 + C_3)}{g_1 (C_2 + C_3) + (g_3 + g_m)\,C_2},$$

$$S_{g_3}^{Q} = \frac{1}{2} - \frac{g_3 C_2}{g_3 C_2 + g_1 (C_2 + C_3) + g_m C_2},$$

$$S_{g_m}^{Q} = -\frac{g_m C_2}{g_1 C_3 + (g_1 + g_3 + g_m) C_2} \tag{8.40}$$

$$S_{C_2}^{K} = -S_{C_3}^{K} = \frac{g_1 C_3}{g_1 C_3 + (g_1 + g_3 + g_m) C_2},$$

$$S_{g_1}^{K} = -\frac{g_1 (C_2 + C_3)}{g_1 C_3 + (g_1 + g_3 + g_m) C_2},$$

$$S_{g_3}^{K} = -\frac{g_3 C_2}{g_1 C_3 + (g_1 + g_3 + g_m) C_2},$$

$$S_{g_m}^{K} = 1 - \frac{g_m C_2}{g_1 C_3 + (g_1 + g_3 + g_m) C_2} \tag{8.41}$$

When $C_1 = C_3 = C$ and $g_2 = g_3 = g$, we have the following simple expressions:

$$S_{C_2}^{\omega_o} = S_{C_3}^{\omega_o} = -S_{g_1}^{\omega_o} = -S_{g_3}^{\omega_o} = -\frac{1}{2}, \quad S_{g_m}^{\omega_o} = 0 \tag{8.42}$$

$$-S_{C_2}^{Q} = S_{C_3}^{Q} = S_{g_3}^{Q} = \frac{1}{2} - Q,$$

$$S_{g_1}^{Q} = \frac{1}{2} - 2Q, \quad S_{g_m}^{Q} = -1 + 3Q \tag{8.43}$$

$$S_{C_2}^{K} = -S_{C_3}^{K} = -S_{g_3}^{K} = Q, \quad S_{g_1}^{K} = -2Q, \quad S_{g_m}^{K} = 3Q \tag{8.44}$$

From the sensitivity results, it can be observed that the design using the circuit in Fig. 8.6(a) with the OTA input terminals interchanged has very low ω_o sensitivity. However, the Q and K sensitivities display a modest Q dependence, although this is no problem for low Q design. The realization of large Q may cause an increase in the sensitivity. But considering that the ω_o sensitivity contributes more to response deviation than the Q sensitivity [47], the design is still useful for not very large Q, since the ω_o sensitivities are extremely low. Also, note that for filter design, the gain sensitivity is of less concern than the ω_o and Q sensitivities. Therefore when commenting the filter sensitivity performance, we mainly consider the ω_o and Q sensitivities.

It is also worthwhile mentioning that in bandpass filter design the design formulas can also be expressed in terms of ω_o and B only and the bandwidth sensitivities can be calculated by using $S_x^B = S_x^{\omega_o} - S_x^Q$. This can be practiced readily for the bandpass filter in Fig. 8.6(a) using the above results.

Another bandpass filter is associated with $Y_1 = g_1 + sC_1$, $Y_2 = sC_2$, $Y_3 = g_3$, shown in Fig. 8.6(b). Its transfer function is given by

$$H_1(s) = \frac{s g_m C_2}{s^2 C_1 C_2 + s\left[g_3 C_1 + (g_1 + g_3 + g_m) C_2\right] + g_1 g_3} \tag{8.45}$$

This filter function is similar to that of the above bandpass filter in Eq. (8.35). Thus similar performances are expected.

8.3 Second-Order Filters Derived from Four-Admittance Model

In this section we consider another two general single-OTA models and filter structures derived from them. We first consider the model in Fig. 8.7, which consists of an OTA and four admittances. This model may be looked upon as a result of grounding the non-inverting terminal of the OTA and applying a voltage input through an admittance to the inverting terminal of the OTA in Fig. 8.1. It can be shown that the transfer function of the new model in Fig. 8.7 is given by

$$H(s) = \frac{Y_1\,(Y_3 - g_m)}{Y_1Y_3 + Y_1Y_4 + Y_2Y_3 + Y_2Y_4 + Y_3Y_4 + g_mY_3} \tag{8.46}$$

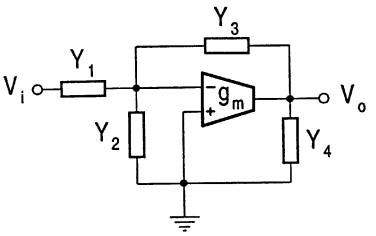

FIGURE 8.7
General model with four admittances.

Similarly, filter structures can be generated by selecting proper components in the model and the corresponding transfer functions can be obtained from Eq. (8.46).

8.3.1 Filter Structures and Design

The filter structures derived from the general model will be presented in this section. We will show how to design the filters to meet given specifications and analyze the corresponding sensitivity performance.

Lowpass Filter

When choosing $Y_1 = g_1, Y_2 = sC_2, Y_3 = g_3, Y_4 = sC_4$, we have a lowpass filter as shown in Fig. 8.8, which has the transfer function

$$H(s) = \frac{g_1(g_3 - g_m)}{s^2C_2C_4 + s\,[g_3C_2 + (g_1 + g_3)\,C_4] + (g_1 + g_m)\,g_3} \tag{8.47}$$

Comparing its transfer function in Eq. (8.47) with the desired function in Eq. (8.15) yields the following equations:

$$\omega_o = \sqrt{\frac{(g_1+g_m)g_3}{C_2C_4}}, \qquad Q = \frac{\sqrt{(g_1+g_m)g_3C_2C_4}}{g_3C_2+(g_1+g_3)C_4},$$

$$K = \frac{g_1g_3-g_1g_m}{g_1g_3+g_3g_m} \tag{8.48}$$

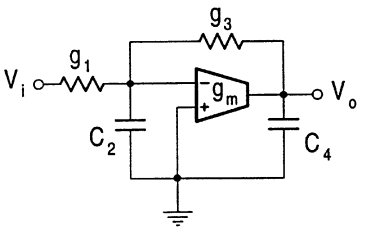

FIGURE 8.8
Lowpass filter derived from Fig. 8.7.

Based on these expressions we can design and analyze the filter. But we want first to draw the reader's attention to the similarity and difference of Eq. (8.22) and Eq. (8.48). The two filters have the same ω_o and Q expressions in form, the difference being only in the subscripts of g_j and C_j, although the gain expressions are different. The same design method can be used and the same design formulas and sensitivity performance of ω_o and Q will be achieved. To show this, we select $C_2 = C_4 = C$ and $g_1 = g_3 = g$. Using Eq. (8.48) we can obtain the design formulas as

$$g = \frac{\omega_o C}{3Q}, \quad g_m = 3Q\omega_o C\left(1 - \frac{1}{9Q^2}\right), \quad K = -\left(1 - \frac{2}{9Q^2}\right) \tag{8.49}$$

and the sensitivity expressions of the filter as

$$S_{C_2}^{\omega_o} = S_{C_4}^{\omega_o} = -S_{g_3}^{\omega_o} = -\frac{1}{2}, \quad S_{g_1}^{\omega_o} = \frac{1}{18Q^2},$$

$$S_{g_m}^{\omega_o} = \frac{1}{2}\left(1 - \frac{1}{9Q^2}\right) \tag{8.50}$$

$$-S_{C_2}^{Q} = S_{C_4}^{Q} = S_{g_3}^{Q} = -\frac{1}{6}, \quad S_{g_1}^{Q} = -\frac{1}{3} + \frac{1}{18Q^2},$$

$$S_{g_m}^{Q} = S_{g_m}^{\omega_o} \tag{8.51}$$

$$S_{C_2}^{K} = S_{C_4}^{K} = 0, \quad S_{g_1}^{K} = 1 - \frac{1}{9Q^2},$$

$$S_{g_3}^{K} = -\frac{1 - \frac{1}{9Q^2}}{1 - \frac{2}{9Q^2}}, \quad S_{g_m}^{K} = \frac{2}{9Q^2}\frac{1 - \frac{1}{9Q^2}}{1 - \frac{2}{9Q^2}} \tag{8.52}$$

Just as we expected, the designed lowpass filter has very low sensitivity and simple design formulas like the filter in Fig. 8.5(a).

Bandpass Filter

A bandpass filter will result for $Y_1 = sC_1$, $Y_2 = g_2$, $Y_3 = g_3$, $Y_4 = sC_4$ as shown in Fig. 8.9(a). The corresponding transfer function is given by

$$H(s) = \frac{s(g_3 - g_m)C_1}{s^2C_1C_4 + s\left[g_3C_1 + (g_2 + g_3)\,C_4\right] + (g_2 + g_m)\,g_3} \tag{8.53}$$

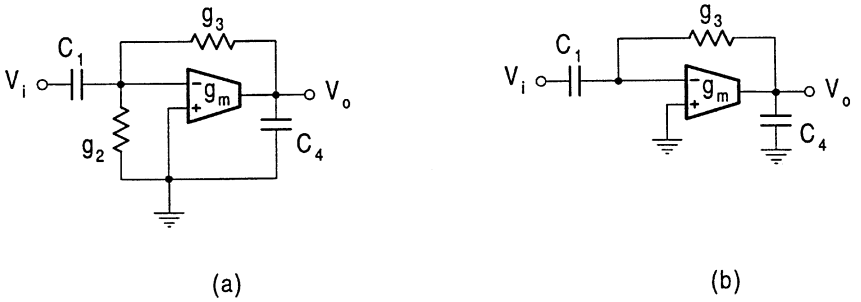

FIGURE 8.9
Bandpass filters derived from Fig. 8.7.

Comparing Eq. (8.53) with Eq. (8.36) leads to

$$\omega_o = \sqrt{\frac{(g_2+g_m)g_3}{C_1C_4}}, \quad Q = \frac{\sqrt{(g_2+g_m)g_3C_1C_4}}{g_3C_1+(g_2+g_3)C_4},$$

$$K = \frac{(g_3-g_m)C_1}{g_3C_1+(g_2+g_3)C_4} \tag{8.54}$$

Setting $C_1 = C_4 = C$ and $g_2 = g_3 = g$, for example, we can obtain g and g_m, being the same as those in Eq. (8.49) of the lowpass filter, but $K = -(9Q^2 - 2)/3$.

As a numerical example, for the bandpass filter of $f_o = 1MHz$ and $Q = 5$ choosing $C = 10pF$ we can determine $g = 4.2\mu S$ and $g_m = 938.3\mu S$. The filter gain is equal to 74.3.

As is obvious from their ω_o and Q expressions, the bandpass filter in Fig. 8.9(a) has the same ω_o and Q sensitivities as those of the lowpass filter in Fig. 8.8. As demonstrated above, these sensitivities are very low, less than or equal to 1/2. The gain sensitivities of the bandpass filter are given below:

$$S_{C_1}^K = -S_{C_4}^K = \frac{2}{3}, \quad S_{g_2}^K = -\frac{1}{3},$$

$$S_{g_3}^K = -\frac{2}{3} + \frac{1}{2-9Q^2}, \quad S_{g_m}^K = \frac{1-9Q^2}{2-9Q^2} \tag{8.55}$$

The gain sensitivities are also as low as those of the lowpass filter in Fig. 8.8.

We must emphasize the attractive low sensitivity feature of the bandpass filter. Especially the sensitivities will become smaller as Q increases, which makes it particularly suitable for large Q applications. Recalling that the bandpass filters generated in Section 8.2.4 are not suitable for large Q applications, because the Q sensitivities are proportional to Q.

Notice that for $g_2 = 0$, the transfer function in Eq. (8.53) becomes

$$H(s) = \frac{s\,(g_3 - g_m)\,C_1}{s^2C_1C_4 + sg_3\,(C_1 + C_4) + g_mg_3} \tag{8.56}$$

This reveals that eliminating the g_2 resistor in Fig. 8.9(a), the circuit can still support the bandpass function. This simplified circuit is given in Fig. 8.9(b).

For the simplified bandpass filter without the g_2 resistor in Fig. 8.9(b), we have

$$\omega_o = \sqrt{\frac{g_m g_3}{C_1 C_4}}, \quad Q = \sqrt{\frac{g_m}{g_3}} \frac{\sqrt{C_1 C_4}}{C_1 + C_4}, \quad K = \frac{(g_3 - g_m) C_1}{g_3 (C_1 + C_4)} \tag{8.57}$$

Selecting $C_1 = C_4 = C$, we can obtain

$$g_3 = \frac{\omega_o C}{2Q}, \quad g_m = 2Q\omega_o C, \quad K = \frac{1}{2}\left(1 - 4Q^2\right) \tag{8.58}$$

which are similar to the formulas in Eq. (8.17) for the lowpass filter in Section 8.2.2.

It can also be observed that the bandpass filter with $g_2 = 0$ in Fig. 8.9(b) has the same ω_o and Q sensitivities as those of the lowpass filter in Section 8.2.2. The gain sensitivities are shown as

$$S_{g_m}^K = -S_{g_3}^K = -\frac{4Q^2}{1 - 4Q^2}, \quad S_{C_1}^K = -S_{C_4}^K = \frac{1}{2} \tag{8.59}$$

which are also low.

Other Considerations on Structure Generation

Throughout this chapter, we are mainly concerned with canonic second-order structures containing only two capacitors. Of course, if more capacitors are used, then more structures may be obtained. For example, if $Y_1 = sC_1$, $Y_2 = sC_2$, $Y_3 = g_3$, $Y_4 = sC_4$, then the bandpass filter in Fig. 8.10(a) will arise, which has the transfer function

$$H(s) = \frac{s (g_3 - g_m) C_1}{s^2 (C_1 + C_2) C_4 + s g_3 (C_1 + C_2 + C_4) + g_m g_3} \tag{8.60}$$

Comparison of Eq. (8.60) with Eq. (8.36) yields ω_o, Q and K expressions, from which design can be carried out. Two design methods are given below. One method is to set $C_1 = C_2 = C_4 = C$. The following formulas are then obtained.

$$g_m = 3Q\omega_o C, \quad g_3 = \frac{2\omega_o C}{3Q}, \quad K = \frac{1}{3} - \frac{3}{2}Q^2 \tag{8.61}$$

The other method is to set $C_1 + C_2 = C_4 = C$ and specify K. This yields

$$g_m = 2Q\omega_o C, \quad g_3 = \frac{\omega_o C}{2Q}, \quad C_1 = \frac{2KC}{1 - 4Q^2}, \quad C_2 = C - C_1 \tag{8.62}$$

From the C_1 formula we can see that for practical Q values ($Q > 1/2$), only negative gain K can be achieved.

It is also possible to obtain other filter configurations by using a combination of more elements for an admittance. For example, if $Y_1 = sC_1$, $Y_2 = g_2$, $Y_3 = g_3 + sC_3$, $Y_4 = g_4$ (two components

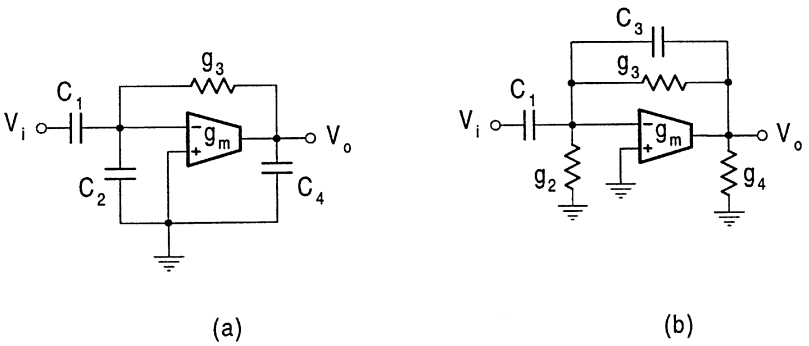

FIGURE 8.10
Bandpass with three capacitors and highpass filter using component matching.

are used for Y_3) as shown in Fig. 8.10(b), we have the transfer function as

$$H(s) = \frac{s^2 C_1 C_3 + sC_1 (g_3 - g_m)}{s^2 C_1 C_3 + s\left[(g_3 + g_4) C_1 + (g_2 + g_4 + g_m) C_3\right] + (g_2 g_3 + g_2 g_4 + g_3 g_4 + g_3 g_m)} \tag{8.63}$$

When $g_3 = g_m$, a highpass filter will result. This realization is however not particularly attractive, due to the use of difference matching. This problem for the highpass filter realization can be overcome by using the models in Section 8.3.2 and Section 8.7.

8.3.2 Second-Order Filters with the OTA Transposed

The second model with four admittances is displayed in Fig. 8.11. This model may be considered as a modification of Fig. 8.1 by grounding the non-inverting terminal of the OTA and applying a voltage input through an admittance to the output node of the OTA. It can also be reckoned as a consequence of transposing the OTA, that is, interchanging the input and output of the OTA in Fig 8.7. The general transfer function of the model can be demonstrated as

$$H(s) = \frac{Y_1 Y_3}{Y_1 Y_3 + Y_1 Y_4 + Y_2 Y_3 + Y_2 Y_4 + Y_3 Y_4 + g_m Y_3} \tag{8.64}$$

Note that the transfer function misses the term of $-g_m$ in the numerator, but has the same denominator compared with the function in Eq. (8.46). As will be seen, the former leads to some advantages such as more filter functions and better programmability while retaining low sensitivity. Also, similar design methods can be used. For example, the capacitances can take the same value and the resistances may be set to be identical. A number of filter configurations can be produced from the model.

Highpass Filter

A highpass characteristic is achieved by setting $Y_1 = sC_1, Y_2 = g_2, Y_3 = sC_3, Y_4 = g_4$. The circuit is shown in Fig. 8.12, with the transfer function given by

$$H(s) = \frac{s^2 C_1 C_3}{s^2 C_1 C_3 + s\left[g_4 C_1 + (g_2 + g_4 + g_m) C_3\right] + g_2 g_4} \tag{8.65}$$

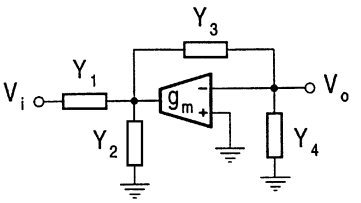

FIGURE 8.11
General four-admittance model with the OTA transposed.

Note that there are no difference nulling conditions involved in this highpass realization which also saves one resistor, compared with the one in Fig. 8.10(b).

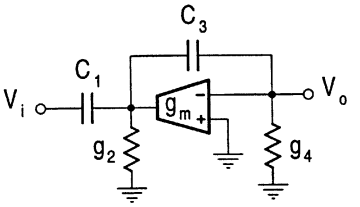

FIGURE 8.12
Highpass filter with transposed OTA.

Design can be carried out by comparing Eq. (8.65) with the standard highpass characteristic

$$H_d(s) = \frac{Ks^2}{s^2 + \frac{\omega_o}{Q}s + \omega_o^2} \tag{8.66}$$

where K is the gain at the infinite frequency, ω_o is the undamped natural frequency, and the quality factor Q relates to the transition sharpness. Design equations are as follows ($K = 1$):

$$\omega_o = \sqrt{\frac{g_2 g_4}{C_1 C_3}}, \qquad Q = \frac{\sqrt{g_2 g_4 C_1 C_3}}{g_4 C_1 + (g_2 + g_4 + g_m) C_3} \tag{8.67}$$

Choosing $C_1 = C_3 = C$ and $g_2 = g_4 = g$ we can determine that

$$g = \omega_o C, \qquad g_m = \frac{\omega_o C}{Q}(1 - 3Q) \tag{8.68}$$

The ω_o and Q sensitivities are similar to those in Section 8.2.4 as can be inspected from the similarity between the two denominators of Eqs. (8.35) and (8.65). From the sensitivity results in Eqs. (8.42) and (8.43). It can be seen that for this design, the highpass circuit has very low ω_o sensitivities, but Q sensitivities will increase with Q. The filter thus may not suit very high Q applications. The design also requires interchanging the OTA input terminals. A highpass filter which has very low Q sensitivity will be presented in Section 8.7.

Lowpass Filter

A lowpass filter is attained by choosing $Y_1 = g_1$, $Y_2 = sC_2$, $Y_3 = g_3$, $Y_4 = sC_4$. The corresponding circuit is exhibited in Fig. 8.13 and its transfer function is given by

$$H(s) = \frac{g_1 g_3}{s^2 C_2 C_4 + s\left[g_3 C_2 + (g_1 + g_3)\, C_4\right] + (g_1 + g_m)\, g_3} \tag{8.69}$$

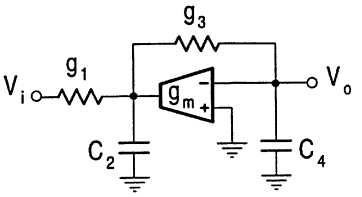

FIGURE 8.13
Lowpass filter with transposed OTA.

The denominator of the transfer function in Eq. (8.69) is the same as that in Eq. (8.47). The design formulas for $C_2 = C_4 = C$ and $g_1 = g_3 = g$ are hence the same as those in Eq. (8.49), with the only difference being $K = 1/9Q^2$. The ω_o and Q sensitivities are also the same as those in Eqs. (8.50) and (8.51), which are very low.

Bandpass Filters

A bandpass filter can be obtained by selecting $Y_1 = sC_1$, $Y_2 = g_2$, $Y_3 = g_3$, $Y_4 = sC_4$ which is shown in Fig. 8.14(a) and has a transfer function as

$$H(s) = \frac{s g_3 C_1}{s^2 C_1 C_4 + s\left[g_3 C_1 + (g_2 + g_3)\, C_4\right] + (g_2 + g_m)\, g_3} \tag{8.70}$$

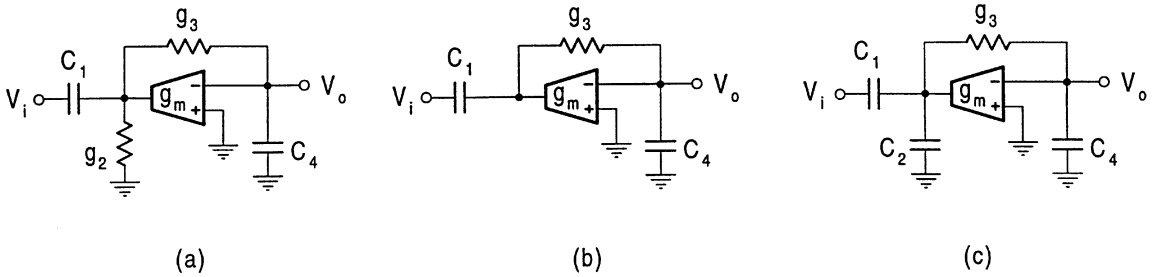

FIGURE 8.14
Bandpass filters with transposed OTA.

One design method is to set $C_1 = C_4 = C$ and $g_2 = g_3 = g$, which gives the formulas the same as those for the bandpass filter in Fig. 8.9(a), as Eqs. (8.70) and (8.53) have exactly the same denominator, but $K = 1/3$. Another method for the bandpass filter design is to set $C_1 = C_4 = C$ only. The filter gain K can then be used as a design parameter. The design formulas are derived as

$$g_3 = K\frac{\omega_o C}{Q}, \quad g_2 = (1 - 2K)\frac{\omega_o C}{Q},$$

$$g_m = \frac{Q\omega_o C}{K}\left[1 - \frac{K(1-2K)}{Q^2}\right] \tag{8.71}$$

The condition is $K < 1/2$ to ensure a positive g_2. When $K = 1/2$, we have

$$g_3 = \frac{\omega_o C}{2Q}, \quad g_2 = 0, \quad g_m = 2Q\omega_o C \tag{8.72}$$

Similar to the discussion in Section 8.3.1, this reveals that the g_2 resistor can be removed. Generally, a simpler bandpass filter can be obtained by removing the g_2 resistor from Fig. 8.14(a), as shown in Fig. 8.14(b). This simple filter has a transfer function

$$H(s) = \frac{sg_3C_1}{s^2C_1C_4 + sg_3(C_1 + C_4) + g_m g_3} \tag{8.73}$$

another circuit which is as simple as the lowpass filter in Fig. 8.4.

A bandpass filter with three capacitors is also obtained by assigning $Y_1 = sC_1$, $Y_2 = sC_2$, $Y_3 = g_3$, $Y_4 = sC_4$ as shown in Fig. 8.14(c). The transfer function is derived as

$$H(s) = \frac{sg_3C_1}{s^2(C_1 + C_2)C_4 + sg_3(C_1 + C_2 + C_4) + g_m g_3} \tag{8.74}$$

With $C_2 = 0$ this circuit will also reduce to Fig. 8.14(b). It should be noted that the bandpass filters in Fig. 8.14 all have very low sensitivities as their counterparts in Section 8.3.1.

The model in Fig. 8.11 can also support another bandpass filter which corresponds to $Y_1 = g_1$, $Y_2 = sC_2$, $Y_3 = sC_3$, $Y_4 = g_4$ as shown in Fig. 8.15. This bandpass filter has a transfer function

$$H(s) = \frac{sg_1C_3}{s^2C_2C_3 + s[g_4C_2 + (g_1 + g_4 + g_m)C_3] + g_1g_4} \tag{8.75}$$

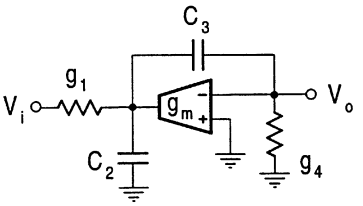

FIGURE 8.15
Another bandpass filter from Fig. 8.11.

Assuming $C_2 = C_3 = C$ we determine g_1, g_4 and g_m in terms of ω_o, Q and K, given by

$$g_1 = K\frac{\omega_o}{Q}, \quad g_4 = \frac{\omega_o Q}{K}, \quad g_m = \frac{\omega_o Q}{K}\left[-2 + \frac{(1-K)K}{Q^2}\right] \tag{8.76}$$

We can also further assign $g_1 = g_4 = g$, which will result in the same g and g_m as those for the highpass filter in Eq. (8.68), but K is fixed to be Q.

8.4 Tunability of Active Filters Using Single OTA

It is well known that the transconductance of an OTA is controllable by the bias dc current or voltage. For instance, the relationship between the transconductance and bias current of the bipolar OTA, CA3080, is given by [9]

$$g_m = \frac{1}{2V_T} I_B \tag{8.77}$$

where V_T is the thermal voltage and has a value of $26mV$ at room temperature. I_B is the bias current. If voltage is preferred to be the controlling variable, then a bias circuit can be used to convert the voltage to the current.

It is obvious that when design has determined g_m, the bias current needed can also be decided by Eq. (8.77), given by

$$I_B = 2V_T g_m \tag{8.78}$$

For example, if $g_m = 19.2mS$, then $I_B = 1mA$.

Programmability is one of the most attractive features of the OTA, since this makes it possible to tune filters electronically, which is especially important for on-chip tuning of fully integrated filters [5, 6, 37, 38, 39, 41, 42]. From the transfer functions of the OTA filters developed, it can be demonstrated that some structures are indeed tunable. For example, the center frequency ω_o of the bandpass filters in Figs. 8.9, 8.10, and 8.14 can be tuned independently of their bandwidth B, while the bandpass filters in Figs. 8.6 and 8.15 have the bandwidth B separately tunable from the center frequency ω_o. The quality factor Q can be controlled independently from the cutoff frequency ω_o for the highpass filter in Fig. 8.12.

8.5 OTA Nonideality Effects

Having considered filter structure generation, design, and sensitivity analysis we can now discuss some of the more practical problems in OTA filter design. In particular we will deal with the effects of OTA nonidealities on filter performance. The methods for the evaluation and reduction of the effects will be proposed.

8.5.1 Direct Analysis Using Practical OTA Macro-Model

It will be recalled from Chapter 3 that an OTA macro-model with finite input and output impedances and transconductance frequency dependence is shown in Fig. 8.16. We use G_i and C_i to represent the differential input conductance and capacitance and drop subscript d (for differential) for simplicity. G_o and C_o are those at the output. The common-mode input conductance G_{ic} and capacitance C_{ic} are ignored because they are usually very small in practice compared with differential counterparts and can be absorbed as most filter structures have a grounded capacitor or a grounded OTA resistor from OTA input terminals to ground. This will be assumed throughout all remaining chapters, unless otherwise stated. The input and output admittances can be written as $Y_i = G_i + sC_i$ and $Y_o = G_o + sC_o$. The transconductance frequency dependence can be described using a single pole model, as mentioned in Chapter 3 and repeated below:

$$g_m(s) = \frac{g_{m0}}{1 + \frac{s}{\omega_b}} \tag{8.79}$$

where ω_b is the finite bandwidth of the OTA and g_{m0} is the dc transconductance. The phase shift model is also often used, which is given, in the frequency domain, by [12]

$$g_m(j\omega) = g_{m0}e^{-j\phi} \tag{8.80}$$

where ϕ is the phase delay. Both models can be approximated as

$$g_m(s) \approx g_{m0}(1 - s\tau) \tag{8.81}$$

where $\tau = 1/\omega_b$ is the time delay and $\phi = \omega\tau$, when $\omega << \omega_b$. In the following the related terminologies may be used alternatively.

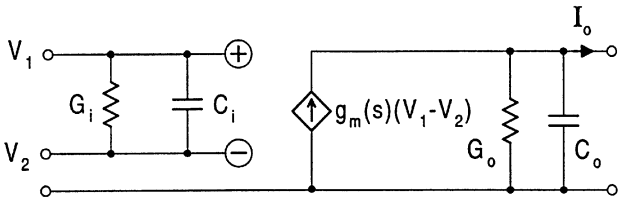

FIGURE 8.16
Practical OTA macro-model.

To give the reader some numerical order of OTA parameter values, a CMOS OTA, for example, may have the following data:

$$g_{m0} = 56\mu S, \quad f_b = 100MHz \ (\tau = 1.59ns), \quad G_i = 0,$$

$$G_o = 1\mu S \ (R_o = 1M\Omega), \ C_i = 0.05pF, \quad C_o = 0.1pF$$

Now we consider the effects of OTA nonidealities on filters in detail. For the circuit in Fig. 8.1, incorporating the OTA macro-model we can derive the following modified transfer function

$$H_1'(s) = \frac{Y_2 g_m(s) + (Y_2 + Y_3 + Y_o)\, Y_i}{(Y_1 + Y_i)\,(Y_2 + Y_3 + Y_o) + Y_2\,(Y_3 + Y_o) + Y_2 g_m(s)} \tag{8.82}$$

Noting that if only the OTA frequency dependence is of concern, the associated transfer function can be simply obtained by substituting $g_m(s)$ for g_m in the ideal expression in Eq. (8.1).

Using the general equation, the impact of the OTA nonidealities on any derived filter structures can be evaluated. Take the lowpass filter in Fig. 8.4 as an example. With finite OTA impedances and bandwidth taken into account, the transfer function of the filter becomes

$$H_1'(s) = K\frac{s^2 + \frac{\omega_z}{Q_z}s + \omega_z^2}{s^2 + \frac{\omega_o'}{Q'}s + \omega_o'^2} \tag{8.83}$$

where

$$\omega_o' = \omega_o\sqrt{\frac{1 + \frac{G_i}{g_{m0}} + \frac{G_o}{g_{m0}}}{1 + \frac{C_i}{C_1} + \frac{C_o}{C_3}}} \tag{8.84}$$

$$Q' = Q\frac{\sqrt{\left(1+\frac{G_i}{g_{m0}}+\frac{G_o}{g_{m0}}\right)\left(1+\frac{C_i}{C_1}+\frac{C_o}{C_3}\right)}}{1+\frac{C_3}{C_1+C_3}\frac{G_i}{g_2}+\frac{C_1}{C_1+C_3}\frac{G_o}{g_2}+\frac{C_i}{C_1+C_3}+\frac{C_o}{C_1+C_3}-\frac{g_{m0}\tau}{C_1+C_3}} \tag{8.85}$$

$$K = \frac{C_3C_i}{C_1C_3+C_3C_i+C_1C_o} \tag{8.86}$$

$$\omega_z = \sqrt{\frac{g_2\left(g_{m0}+G_i\right)}{C_3C_i}} \tag{8.87}$$

$$Q_z = \frac{\sqrt{g_2\left(g_{m0}+G_i\right)C_3C_i}}{g_2C_i+C_3G_i-g_{m0}g_2\tau} \tag{8.88}$$

Note that K is the gain at the infinity frequency, that is, $H_1'(\infty) = K$. The dc gain can be derived as

$$H_1'(0) = H_1(0)\frac{1+\frac{G_i}{g_{m0}}}{1+\frac{G_i}{g_{m0}}+\frac{G_o}{g_{m0}}} \tag{8.89}$$

In the above equations, ω_o and Q are as shown in Eq. (8.16). $H_1(0)$ represents the ideal dc gain, which is unity.

During the formulation of Eq. (8.83), for simplicity and without loss of insight into the problem, we use a first-order approximation. The first glance at the equation indicates that the ideal all-pole lowpass function in Eq. (8.14), now becomes a general biquadratic function with finite transmission zeros and all coefficients are changed.

Of all the parasitics contributing to the change of the transfer function, the input and output conductances (especially the latter) seem to have greater influence on the low frequency response than others and introduce losses causing reduction of the pole and zero quality factors and the low-frequency gain. For example, the dc gain in Eq. (8.89) is totally dependent on the finite conductances, being less than unity. The finite input and output capacitances affect more the high-frequency response. At the extreme infinite frequency the magnitude, as shown in Eq. (8.86), is no longer zero, but a finite value determined completely by the nonideal capacitances, especially the input capacitance. Note in particular that the input conductance and capacitance provide extra signal paths, as can be seen from the numerator parameters. Therefore the differential input application of the OTA may not be favorable in some cases.

Two major effects of $g_m(s)$ should be emphasized. From the pole quality factor Q' expression in Eq. (8.85), we can see that transconductance frequency dependence can enhance the Q, which is known as the Q enhancement effect. The other is the stability problem, that is, the finite ω_b may cause the circuit to oscillate by shifting the poles to the right plane.

To appreciate the change more clearly, we further write the parameters in the relative change form (a first-order approximation is adopted during the whole simplification). Using Eq. (8.84) and denoting $\Delta\omega_o = \omega_o' - \omega_o$ we can obtain

$$\frac{\Delta\omega_o}{\omega_o} = \frac{1}{2}\left(\frac{G_i}{g_{m0}}+\frac{G_o}{g_{m0}}-\frac{C_i}{C_1}-\frac{C_o}{C_3}\right) \tag{8.90}$$

In a similar way, from Eq. (8.85) and with $\Delta Q = Q' - Q$ we have

$$\frac{\Delta Q}{Q} = \left(\frac{1}{2g_{m0}} - \frac{1}{g_2}\frac{C_3}{C_1+C_3}\right)G_i + \left(\frac{1}{2g_{m0}} - \frac{1}{g_2}\frac{C_1}{C_1+C_3}\right)G_o$$
$$+ \frac{g_{m0}}{C_1+C_3}\tau + \frac{C_3-C_1}{2C_1(C_1+C_3)}C_i + \frac{C_1-C_3}{2C_3(C_1+C_3)}C_o \tag{8.91}$$

Finally, from Eq. (8.89) and with $\Delta H_1(0) = H_1'(0) - H_1(0)$ we can derive

$$\frac{\Delta H_1(0)}{H_1(0)} = -\frac{G_o}{g_{m0}} \tag{8.92}$$

Equation (8.90) clearly shows that G_i and G_o increase ω_o, while C_i and C_o decrease ω_o. The excess phase has no effect on ω_o (for the first-order approximation). Equation (8.92) reveals that G_o has a reduction impact on the dc gain. The effects on Q depend on how the circuit is designed. For the design in Section 8.2.2, with normalized $C_1 = C_3 = C = 1F$, Eq. (8.91) reduces to

$$\frac{\Delta Q}{Q} = \frac{g_2 - g_{m0}}{2g_{m0}g_2}(G_i + G_o) + \frac{g_{m0}}{2}\tau \tag{8.93}$$

Further substituting the design formulas in Eq. (8.17) with $C = 1F$ gives

$$\frac{\Delta Q}{Q} = \frac{1-4Q^2}{4\omega_o Q}(G_i + G_o) + Q\omega_o\tau \tag{8.94}$$

Therefore, τ has a Q enhancement effect. C_i and C_o have no impact on Q for the first-order approximation and $C_1 = C_3$. G_i and G_o will cause Q reduction. We should stress that the contribution of excess phase ($\phi = \omega_o\tau$) to the Q enhancement is multiplied by Q^2, that is ΔQ(due to ϕ)$= Q^2\phi$, as can be seen from Eq (8.94). Therefore, for large Q applications, even a very small phase shift can cause a very big increase in Q and thus instability. From this example we also see that a good design can reduce nonideality effects. In particular, using equal design capacitances also reduces the influence of finite OTA input and output capacitances on the pole quality factor, besides the benefits mentioned in Section 8.2.2 such as the zero sensitivities of Q to the capacitances.

It should also be noted that OTAs using different IC technologies may have different performances. For instance, MOS and CMOS OTAs have a very large input resistance, which may thus be assumed infinite in most cases. However, the input resistance of bipolar OTAs is quite low. The above analysis is general, which could be simplified for the CMOS OTA by dropping off G_i, for example.

Similarly, taking the OTA nonidealities into consideration, the general transfer functions of Figs. 8.7 and 8.11 become, respectively,

$$H'(s) = \frac{Y_1(Y_3 - g_m(s))}{\begin{array}{r}Y_1Y_3+Y_1(Y_4+Y_o)+(Y_2+Y_i)Y_3+(Y_2+Y_i)(Y_4+Y_o)\\ +Y_3(Y_4+Y_o)+Y_3g_m(s)\end{array}} \tag{8.95}$$

and

$$H'(s) = \frac{Y_1Y_3}{\begin{array}{r}Y_1Y_3+Y_1(Y_4+Y_i)+(Y_2+Y_o)Y_3+(Y_2+Y_o)(Y_4+Y_i)\\ +Y_3(Y_4+Y_i)+Y_3g_m(s)\end{array}} \tag{8.96}$$

Using the respective equation we can analyze the influence of OTA nonidealities on the filters derived from the general models in Figs. 8.7 and 8.11. The difference of the two expressions in terms of Y_i and Y_o is due to the different connection of the OTA in the models.

8.5.2 Simple Formula Method

A simple method for evaluation of the effects of finite bandwidth has been proposed in Ref. [46]. This method uses the sensitivity to the amplifier gain to assess the effects of phase shift, which simplifies the analysis. Using this method we can, for example, assess the influence of the OTA finite bandwidth on the filter. The associated formulas are given below:

$$\frac{\Delta\omega_o}{\omega_o} = \frac{\omega_o}{2Q\omega_b}\left(S_{g_m}^{\omega_o} - S_{g_m}^{Q}\right) \tag{8.97}$$

$$\frac{\Delta Q}{Q} = \frac{\omega_o}{2Q\omega_b}\left[\left(4Q^2 - 1\right) S_{g_m}^{\omega_o} + S_{g_m}^{Q}\right] \tag{8.98}$$

For the simple lowpass structure in Fig. 8.4, $S_{g_m}^{\omega_o} = S_{g_m}^{Q} = \frac{1}{2}$, as given in Eqs. (8.19) and (8.20). It can be shown that the effect of the finite bandwidth ω_b of the OTA is to cause fractional deviations in Q and ω_o, given approximately by

$$\frac{\Delta\omega_o}{\omega_o} = 0, \qquad \frac{\Delta Q}{Q} = Q\frac{\omega_o}{\omega_b} \tag{8.99}$$

Recognizing that it is deviations in ω_o which frequently cause the greatest deviation in the amplitude response of the filter (see Section 4.4), another attractive feature of this filter is observed from the result. Equation (8.99) can also be derived from Eqs. (8.90) and (8.94), as expected.

Similarly, for the lowpass filter in Fig. 8.8, using the results of $S_{g_m}^{\omega_o}$ and $S_{g_m}^{Q}$ in Eqs. (8.50) and (8.51), we have

$$\frac{\Delta\omega_o}{\omega_o} = 0, \qquad \frac{\Delta Q}{Q} = \frac{Q\omega_o}{\omega_b}\left(1 - \frac{1}{9Q^2}\right) \tag{8.100}$$

8.5.3 Reduction and Elimination of Parasitic Effects

It is possible to reduce the effects of OTA input and output impedances by absorption and those of transconductance frequency dependence by phase lead compensation. To show the former we consider the second-order filter model in Fig. 8.7. The latter will be handled in Chapter 9.

From Eq. (8.95) we can see that if Y_2 and Y_4 are a parallel of a resistor and a capacitor, that is, $Y_2 = g_2 + sC_2$, and $Y_4 = g_4 + sC_4$, then the effects of Y_i and Y_o can be completely eliminated by absorption design, that is, G_i and C_i are absorbed by g_2 and C_2, respectively, and G_o and C_o by g_4 and C_4. Figure 8.17 shows the lowpass circuit which can absorb the OTA input and output impedances and all node parasitic capacitances. The circuit has the following ideal transfer function:

$$H(s) = \frac{g_1\left(g_3 - g_m\right)}{\begin{array}{l}s^2C_2C_4 + s[(g_3+g_4)C_2 + (g_1+g_2+g_3)C_4] \\ \quad + (g_1g_3 + g_1g_4 + g_2g_3 + g_2g_4 + g_3g_4 + g_mg_3)\end{array}} \tag{8.101}$$

For the circuit in Fig. 8.17, the OTA finite conductances and capacitances cause a change in design capacitances and conductances as

$$\Delta C_2 = C_i, \quad \Delta C_4 = C_o, \quad \Delta g_2 = G_i, \quad \Delta g_4 = G_o$$

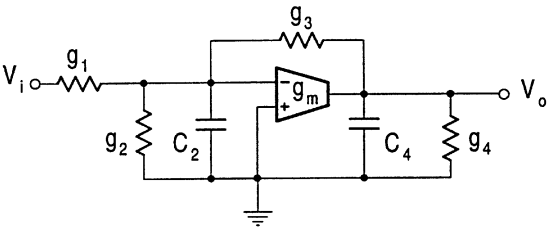

FIGURE 8.17
Lowpass filter that can absorb all parasitic resistances and capacitances.

The absorption approach determines the real component values by subtracting the nominal values with the increments due to nonideal OTA parameters, that is

$$C_{\text{real}} = C_{\text{nominal}} - \Delta C, \quad g_{\text{real}} = g_{\text{nominal}} - \Delta g \tag{8.102}$$

This requires that

$$C_{\text{nominal}} > \Delta C, \quad g_{\text{nominal}} > \Delta g$$

For example, the nominal values for relevant capacitances and conductances must be much bigger than the respective parasitic values. It should be noted that at very high frequencies this may not be always met.

Similar methods for the elimination of the effects of finite OTA input and output impedances can also be discussed based on Eq. (8.96) for the filters derived from Fig. 8.11.

In most cases in this chapter each admittance is treated as a single component, resistor or capacitor. Only in the cases in which we want to achieve additional functions or performances do we consider them as a combination of two components. This will also be the case for the remaining sections of the chapter.

8.6 OTA-C Filters Derived from Single OTA Filters

In the above, many interesting filters using a single OTA have been developed. These single OTA filter structures may not be fully integratable and fully programmable due to the fact that they contain resistors and use only one OTA. But they are still useful for monolithic implementation, because by replacing the discrete resistor with the simulated OTA resistor, they can be very easily converted into the counterparts using OTAs and capacitors only. The derived OTA-C filters should be suitable for full integration. In the following we first discuss how to simulate resistors using OTAs only and then selectively illustrate some OTA-C filters thus derived from the single OTA counterparts.

8.6.1 Simulated OTA Resistors and OTA-C Filters

Resistors can be simulated using OTAs. Figure 8.18(a) shows a simple single OTA connection. This circuit is equivalent to a grounded resistor with resistance equal to the inverse of the OTA transconductance, that is, $R = 1/g_m$ [12]. Floating resistor simulation may require more OTAs. Figure 8.18(b) shows a circuit with two identical OTAs [15]. It can be shown that it is equivalent to a floating resistor of resistance equal to $R = 1/g_m$. Finally, for the ideal voltage input, the first OTA in the input terminated floating resistor simulation is redundant and can thus be eliminated, as

shown in Fig. 8.18(c). This simulation not only saves one OTA but also has a high input impedance, a feature useful for cascade design.

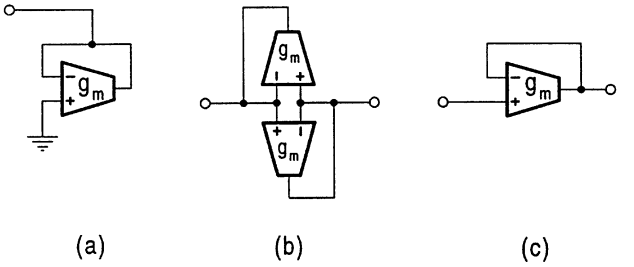

FIGURE 8.18
OTA simulation of resistors.

For simplicity from now on throughout the remaining chapters we will drop subscript m off transconductance g_m in almost all cases except when for some special cases in which the subscript m must be used. The reader should keep in mind that in OTA-C filters, g really means g_m since only OTA and capacitors are used. The function of resistors is simulated by OTAs as discussed above.

We now derive OTA-C filters from some single OTA filters using the resistor substitution method. To stress that they are based on single OTA filter prototypes we keep the g_m symbol for this OTA. A lowpass OTA-C filter is obtained from Fig. 8.4, by simply replacing the floating resistor by the OTA equivalent in Fig. 8.18(b), which is depicted in Fig. 8.19(a). Figure 8.19(b) shows the OTA-C bandpass filter derived from Fig. 8.6(a) using the OTA grounded resistor in Fig. 8.18(a). We give the OTA-C equivalents of the lowpass filter in Fig. 8.8 and the bandpass filter in Fig. 8.9(a), as shown in Figs 8.19(c) and 8.19(d), respectively. The lowpass OTA-C filter in Fig. 8.19(c) uses an input terminated OTA resistor in Fig. 8.18(c) and the grounded OTA resistor in Fig. 8.18(a). The bandpass OTA-C filter in Fig. 8.19(d) consists of an OTA grounded resistor and an OTA floating resistor. The single OTA bandpass filter in Fig. 8.15 and the highpass filter in Fig. 8.12 are also converted into the OTA-C counterparts, which are shown in Figs. 8.19(e) [36] and 8.19(f), respectively.

8.6.2 Design Considerations of OTA-C Structures

The transfer functions of the OTA-C filters are the same as those of the single OTA counterparts. The difference is only that in OTA-C filters, the gs are all OTA transconductances. The resistor substitution method also retains the sensitivity property of the original single OTA filter. Therefore the structures that have minimum sensitivity should be first considered in OTA-C realization. It is evident that the number of OTAs in the derived OTA-C filters will depend on how many resistors are in the original circuits. The architectures with fewer resistors may be attractive in the sense of reducing the number of OTAs. Also, note that the grounded resistor needs fewer OTAs to simulate than the floating resistor, and thus the single OTA filter structures using grounded resistors may be preferable in terms of reduction in the number of OTAs in the derived OTA-C filters. As will be discussed immediately, the grounded resistor will also introduce fewer parasitic elements into the filter circuit than the floating resistor when the nonidealities of the OTA(s) simulating them are taken into consideration. It should also be noted that structures using grounded capacitors are advantageous with respect to reducing parasitic effects and the chip area, as the floating capacitor has bigger parasitic capacitances and requires larger chip area.

For the OTA-RC filters we have discussed the effects of nonidealities of the OTA g_m. When dealing with the OTA-C equivalent we must also consider the nonidealities of the OTAs simulating resistors. For the grounded OTA resistor in Fig. 8.18(a), the equivalent grounded admittance due to the OTA nonidealities can be demonstrated as (to be general, we include the OTA common-mode

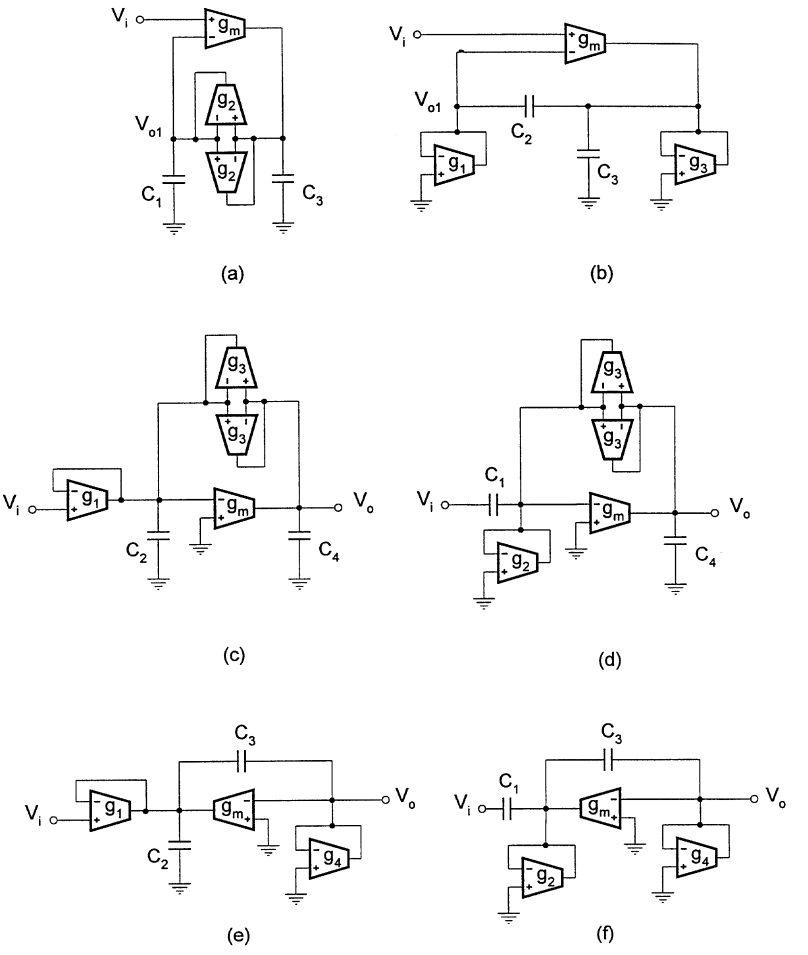

FIGURE 8.19
Examples of OTA-C filters derived from single OTA counterparts.

impedance)

$$Y_{GR} = Y_{id} + Y_{ic} + Y_o + g_m(s) = (G_{id} + G_{ic} + G_o + g_{m0}) + s\,(C_{id} + C_{ic} + C_o - g_{m0}/\omega_b) \tag{8.103}$$

which is a complex admittance, no longer a pure conductance.

For the floating resistor simulation in Fig. 8.18(b), the nonidealities of the two identical OTAs will have more complex effects. We can draw the equivalent circuit taking the OTA nonidealities into account and use the current source shift theorem (in a loop) to simplify the equivalent circuit. The resulting circuit can be further proved to be equivalent to a π type admittance network with the series arm admittance given by

$$Y_{FR\pi s} = 2Y_{id} + g_m(s) = (2G_{id} + g_{m0}) + s\,(2C_{id} - g_{m0}/\omega_b) \tag{8.104}$$

and the two equal parallel arm admittances, given by

$$Y_{FR\pi p} = 2Y_{ic} + Y_o = (2G_{ic} + G_o) + s\,(2C_{ic} + C_o) \tag{8.105}$$

Unlike the grounded resistor, in this case it is impossible to write an equivalent floating admittance.

Now we can consider the effects on OTA-C filters of the nonidealities from the resistor simulation OTAs. For example, in the lowpass OTA-C filter in Fig. 8.19(a) the two identical OTAs simulating the floating resistor of conductance g_2 will have a π equivalent circuit due to their nonidealities as shown above. As can be seen from the circuit structure and the expressions of the series and parallel arm admittances of the π network in Eqs. (8.104) and (8.105), respectively, the finite differential input conductances ($2G_{id2}$) can be absorbed by transconductance g_{20} and the common-mode capacitances and output capacitance ($2C_{ic2} + C_{o2}$) can also be absorbed by C_1 and C_3. But the effects of the finite differential input capacitances and the finite bandwidth will produce a parasitic floating capacitance equal to $2C_{id2} - g_{20}/\omega_{b2}$, and the effect of the common-mode input conductances and the output conductance will generate two parasitic grounded resistors of equal conductances of $2G_{ic2} + G_{o2}$ in parallel with C_1 and C_3. Such parasitic elements will affect the filter poles and zeros. Further analysis can be easily carried out by substituting

$$Y_1' = (2G_{ic2} + G_{o2}) + s\,[C_1 + (2C_{ic2} + C_{o2})]$$

$$Y_3' = (2G_{ic2} + G_{o2}) + s\,[C_3 + (2C_{ic2} + C_{o2})]$$

$$Y_2' = (2G_{id2} + g_{20}) + s\,(2C_{id2} - g_{20}/\omega_{b2})$$

for Y_1, Y_3 and Y_2 in Eq. (8.1). The reader may formulate the corresponding practical expression of the transfer function and compare it with the ideal one in Eq. (8.14) to study the effects in details.

As a second example, the bandpass OTA-C filter with two grounded OTA resistors in Fig. 8.19(b) is considered. Taking the nonidealities of the g_1 and g_3 OTAs into account and using Eq. (8.103) we have the changed grounded admittances as

$$Y_1' = [(G_{id1} + G_{ic1} + G_{o1}) + g_{10}] + s\,(C_{id1} + C_{ic1} + C_{o1} - g_{10}/\omega_{b1})$$

$$Y_3' = [(G_{id3} + G_{ic3} + G_{o3}) + g_{30}] + s\,[C_3 + (C_{id3} + C_{ic3} + C_{o3} - g_{30}/\omega_{b3})]$$

It can be seen that the finite conductances can be absorbed by the respective transconductances of the g_1 and g_3 OTAs. Also, the finite capacitances and bandwidth of the g_3 OTA can be absorbed by C_3. But a parasitic capacitor from the output node to ground will be produced by the finite capacitances and bandwidth of the g_1 OTA, which cannot be absorbed. Again a detailed evaluation can be conducted by substituting Y_1' and Y_3' for Y_1 and Y_3 in Eq. (8.1) and comparing the resulting equation with the ideal transfer function in Eq. (8.35). For example, if only the finite capacitances and bandwidth of the g_1 OTA are considered, we can readily demonstrate that their effect is to produce extra terms in the denominator of the transfer function in Eq. (8.35), which are

$$\left[s^2\,(C_2 + C_3) + sg_3\right](C_{id1} + C_{ic1} + C_{o1} - g_{10}/\omega_{b1})$$

The nonideality effects of the input termination OTA can also be similarly evaluated. The reader may, for example, consider the g_1 OTA in the lowpass circuit in Fig. 8.19(c).

Tuning may need reconsideration. As we have already found in Section 8.4, it is not possible to tune the frequency and quality factor independently in some single OTA filters. By replacing fixed resistors by tunable OTAs the programmability can be enhanced. For instance, the single OTA bandpass filter in Fig. 8.9(a) has only ω_o tunable, while the OTA-C simulation in Fig. 8.19(d) has also tunable B. The tuning process simply involves the tuning of B by the g_2 or g_3 OTA, followed by the adjusting of ω_o by the g_m OTA. It is noted that in the original single OTA bandpass circuit in Fig. 8.15, only the bandwidth or the quality factor is tunable, but now the OTA-C derivative in Fig. 8.19(e) has also the tunable center frequency, as can be seen from Eq. (8.75). We can first tune ω_o by the g_1 or g_4 OTA and then B or Q by the g_m OTA. The final example is the highpass OTA-C filter in Fig. 8.19(f), whose ω_o can be tuned by the g_2 or g_4 OTA and Q then by the g_m OTA, compared with the single OTA prototype in Fig. 8.12 which has only Q electronically adjustable.

8.7 Second-Order Filters Derived from Five-Admittance Model

In this section a more complex one OTA and five-admittance model is considered. The general model with complete feedback is shown in Fig. 8.20. This will be seen to be a development for Fig. 8.1 with two additional admittances. Because more admittances are used, more filter structures and design flexibility can be achieved.

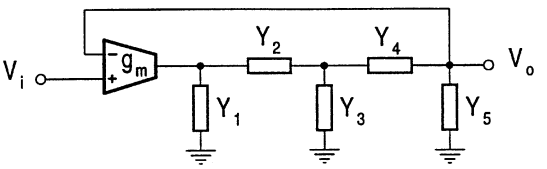

FIGURE 8.20
Five-admittance model with complete output feedback.

The circuit transfer function can be shown as

$$H(s) = \frac{g_m Y_2 Y_4}{\begin{array}{r} Y_1Y_2Y_4+Y_1Y_2Y_5+Y_1Y_3Y_4+Y_1Y_3Y_5+Y_1Y_4Y_5 \\ +Y_2Y_3Y_4+Y_2Y_3Y_5+Y_2Y_4Y_5+g_mY_2Y_4 \end{array}} \tag{8.106}$$

Different filter characteristics can be realized using the general model. This can be done by trying different combinations of passive components in Eq. (8.106). Suppose that each admittance is realized with one element. Exhaustive search shows that a total of 13 different structures can be derived: one highpass, four bandpass and three lowpass filters with five passive components; two bandpass and two lowpass filters with four passive components; as well as one lowpass filter with three passive components. The combinations of components for the 13 structures are presented in Table 8.1. The corresponding configurations and transfer functions can be derived from the general model in Fig. 8.20 and the general expression in Eq. (8.106), which will be presented in the following. These filter structures are suitable for cascade design due to their high input impedance. Note that the four passive element lowpass and bandpass filters derived are actually the same as the counterparts in Figs. 8.5 and 8.6. The three passive component lowpass filter is the same as that in Fig. 8.4. This is no surprise, as the general three-admittance model with output V_{o1} in Fig. 8.1 can be derived from the five-admittance model in the above. We therefore will not repeat them here, although the reader

is encouraged to check this. In the following we will concentrate on the filters with five passive components. These filters can realize the lowpass, highpass, and bandpass functions.

Table 8.1 Generation of Filter Structures Based on Model in Fig. 8.20

Type	Components					Circuit Figure	Function Equation
General	Y_1	Y_2	Y_3	Y_4	Y_5	8.20	8.106
HP	g_1	sC_2	g_3	sC_4	g_5	8.21	8.108
BP1	g_1	sC_2	sC_3	g_4	g_5	8.22(a)	8.113
BP2	g_1	g_2	sC_3	sC_4	g_5	8.22(b)	8.117
BP3	g_1	sC_2	g_3	g_4	sC_5	8.22(c)	8.118
BP4	sC_1	g_2	g_3	sC_4	g_5	8.22(d)	8.119
BP5∗	g_1	∞	sC_3	sC_4	g_5	8.6(a)	8.35
BP6∗	g_1	sC_2	sC_3	∞	g_5	8.6(b)	8.45
LP1	sC_1	g_2	sC_3	g_4	g_5	8.23(a)	8.120
LP2	g_1	g_2	sC_3	g_4	sC_5	8.23(b)	8.122
LP3	sC_1	g_2	g_3	g_4	sC_5	8.23(c)	8.123
LP4∗	g_1	∞	sC_3	g_4	sC_5	8.5(a)	8.21
LP5∗	sC_1	g_2	sC_3	∞	g_5	8.5(b)	8.34
LP6∗	sC_1	g_2	sC_3	∞	0	8.4	8.14

∗ Note that the symbol subscriptions used here are different from those in Section 8.2.

8.7.1 Highpass Filter

A highpass filter can be obtained by selecting $Y_1 = g_1$, $Y_2 = sC_2$, $Y_3 = g_3$, $Y_4 = sC_4$, $Y_5 = g_5$ as shown in Fig. 8.21.

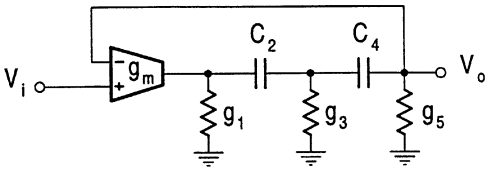

FIGURE 8.21
Highpass filter derived from Fig. 8.20.

We first manipulate Eq. (8.106) according to Y_2 and Y_4 into

$$H(s) = \frac{g_m Y_2 Y_4}{(Y_1 + Y_3 + Y_5 + g_m) Y_2 Y_4 + (Y_1 + Y_3) Y_5 Y_2 + Y_1 (Y_3 + Y_5) Y_4 + Y_1 Y_3 Y_5} \tag{8.107}$$

The transfer function is then easily derived as

$$H(s) = \frac{s^2 g_m C_2 C_4}{s^2 (g_1 + g_3 + g_5 + g_m) C_2 C_4 + s [(g_1 + g_3) g_5 C_2 + g_1 (g_3 + g_5) C_4] + g_1 g_3 g_5} \tag{8.108}$$

Comparison of Eqs. (8.108) and (8.66) will give rise to design equations of ω_o, Q, and K in terms of gs and Cs. Using these equations we can determine component values and analyze sensitivity performance. For the setting up of $C_2 = C_4 = C$ and $g_1 = g_3 = g_5 = g$ we can obtain the component values as

$$g = 4Q\omega_o C, \quad g_m = 64Q^3\omega_o C\left(1 - \frac{3}{16Q^2}\right), \quad K = 1 - \frac{3}{16Q^2} \tag{8.109}$$

and the sensitivities of the design as

$$S_{g1}^{\omega_o} = S_{g3}^{\omega_o} = S_{g5}^{\omega_o} = \frac{1}{2}\left(1 - \frac{1}{16Q^2}\right),$$

$$S_{g_m}^{\omega_o} = -\frac{1}{2}\left(1 - \frac{3}{16Q^2}\right), \quad S_{C_2}^{\omega_o} = S_{C_4}^{\omega_o} = -\frac{1}{2} \tag{8.110}$$

$$S_{g1}^{Q} = S_{g5}^{Q} = -\frac{1}{4}\left(1 - \frac{1}{8Q^2}\right), \quad S_{g3}^{Q} = \frac{1}{32Q^2},$$

$$S_{g_m}^{Q} = \frac{1}{2}\left(1 - \frac{3}{16Q^2}\right), \quad S_{C_2}^{Q} = S_{C_4}^{Q} = 0 \tag{8.111}$$

$$S_{C_2}^{K} = S_{C_4}^{K} = 0, \quad S_{g_m}^{K} = \frac{3}{16Q^2},$$

$$S_{g1}^{K} = S_{g3}^{K} = S_{g5}^{K} = -\frac{1}{16Q^2} \tag{8.112}$$

The sensitivities of the filter are extremely low, the maximum value being $1/2$. Recalling the highpass filter in Section 8.3.2 which has large Q sensitivities for high Q design, the above highpass filter has the advantage of being suitable for any practical Q values in term of sensitivity.

The highpass filter in Fig. 8.21 contains two floating capacitors and three grounded resistors which will determine its performance to the OTA nonidealities and circuit parasitics, which will be discussed with comparison with other filter structures in Section 8.7.4.

A 100 kHz highpass filter is now designed which has a normalized characteristic of

$$H_d(s) = \frac{s^2}{s^2 + 0.5s + 1}$$

which reveals that $Q = 2$. Let $C_2 = C_4 = 10pF$. We can obtain $g_1 = g_3 = g_5 = 50.265\mu S$ and $g_m = 3.066mS$. The designed filter will have a gain of $K = 0.953$.

8.7.2 Bandpass Filter

Four bandpass filter structures are presented in this section. The first bandpass filter is derived from Fig. 8.20 by setting $Y_1 = g_1$, $Y_2 = sC_2$, $Y_3 = sC_3$, $Y_4 = g_4$, $Y_5 = g_5$ as shown in Fig. 8.22(a).

The transfer function can be found, by sorting out Eq. (8.106) according to Y_2 and Y_3, as

$$H(s) = \frac{s g_m g_4 C_2}{s^2 (g_4 + g_5) C_2 C_3 + s \{[g_1 (g_4 + g_5) + g_4 (g_5 + g_m)] C_2 + g_1 (g_4 + g_5) C_3\} + g_1 g_4 g_5} \tag{8.113}$$

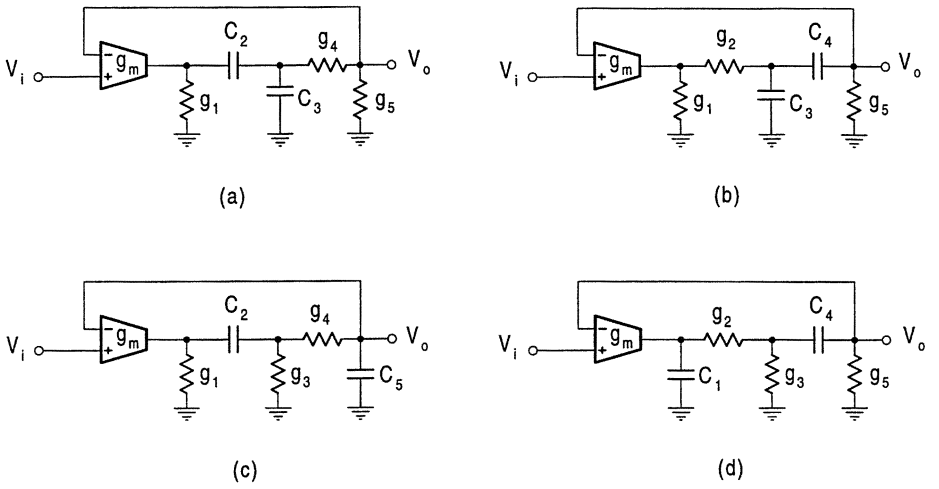

FIGURE 8.22
Four bandpass filters derived from Fig. 8.20.

Similarly we can also derive the design formulas and sensitivity results for this circuit. When $C_2 = C_3 = C$ and $g_1 = g_4 = g_5 = g$, the design formulas are found to be

$$g = \sqrt{2}\omega_o C, \quad g_m = \sqrt{2}\omega_o C \left(-5 + \frac{\sqrt{2}}{Q}\right),$$

$$K = \frac{Q}{\sqrt{2}} \left(-5 + \frac{\sqrt{2}}{Q}\right) \tag{8.114}$$

The OTA input terminals should be interchanged for practical Q values. The sensitivities are derived as

$$S_{g_m}^{\omega_o} = 0, \quad S_{g4}^{\omega_o} = S_{g5}^{\omega_o} = \frac{1}{4}, \quad S_{g1}^{\omega_o} = -S_{C_2}^{\omega_o} = -S_{C_3}^{\omega_o} = \frac{1}{2} \tag{8.115}$$

$$S_{g_m}^{Q} = -\frac{Q}{\sqrt{2}} \left(-5 + \frac{\sqrt{2}}{Q}\right), \quad S_{g4}^{Q} = -\frac{1}{4} + \sqrt{2}Q, \quad S_{g5}^{Q} = \frac{3}{4} - \frac{3Q}{\sqrt{2}},$$

$$S_{g1}^{Q} = \frac{1}{2} - 2\sqrt{2}Q, \quad -S_{C_2}^{Q} = S_{C_3}^{Q} = \frac{1}{2} - \sqrt{2}Q \tag{8.116}$$

The second bandpass filter structure is shown in Fig. 8.22(b), which corresponds to $Y_1 = g_1$, $Y_2 =$

$g_2, Y_3 = sC_3, Y_4 = sC_4, Y_5 = g_5$. The transfer function is given by

$$H(s) = \frac{sg_m g_2 C_4}{s^2 (g_1 + g_2) C_3 C_4 + s \{(g_1 + g_2) g_5 C_3 + [(g_1 + g_2) g_5 + (g_1 + g_m) g_2] C_4\} + g_1 g_2 g_5} \tag{8.117}$$

Comparing Eq. (8.117) with Eq. (8.113) we can see that the bandpass filters in Figs. 8.22(a) and (b) have similar transfer functions and therefore similar design procedures and sensitivity performance.

The third bandpass filter with $Y_1 = g_1, Y_2 = sC_2, Y_3 = g_3, Y_4 = g_4, Y_5 = sC_5$ is revealed in Fig. 8.22(c). The fourth bandpass filter corresponding to the choice of $Y_1 = sC_1, Y_2 = g_2, Y_3 = g_3, Y_4 = sC_4, Y_5 = g_5$ is drawn in Fig. 8.22(d). These two bandpass filters have similar transfer functions. The transfer function of Fig. 8.22(c) is formulated as

$$H(s) = \frac{sg_m g_4 C_2}{s^2 (g_1 + g_3 + g_4) C_2 C_5 + s [(g_1 + g_3 + g_m) g_4 C_2 + g_1 (g_3 + g_4) C_5] + g_1 g_3 g_4} \tag{8.118}$$

and the transfer function of Fig. 8.22(d) is given by

$$H(s) = \frac{sg_m g_2 C_4}{s^2 (g_2 + g_3 + g_5) C_1 C_4 + s [(g_2 + g_3) g_5 C_1 + g_2 (g_3 + g_5 + g_m) C_4] + g_2 g_3 g_5} \tag{8.119}$$

It can be shown that all the bandpass filters in Fig. 8.22 have similar sensitivity performance. Also they contain one grounded and one floating capacitor and one floating and two grounded resistors. The OTA-C equivalents will have similar performances to the nonidealities of the g_m OTA and the OTAs simulating the resistors. Section 8.7.4 will further discuss these issues.

8.7.3 Lowpass Filter

Three lowpass filter configurations are now generated. The first lowpass filter is obtained by selecting $Y_1 = sC_1, Y_2 = g_2, Y_3 = sC_3, Y_4 = g_4, Y_5 = g_5$. Substitution into Eq. (8.106) leads to

$$H(s) = \frac{g_m g_2 g_4}{s^2 (g_4 + g_5) C_1 C_3 + s [(g_2 g_4 + g_2 g_5 + g_4 g_5) C_1 + (g_2 g_4 + g_2 g_5) C_3] + g_2 g_4 (g_m + g_5)} \tag{8.120}$$

which compares to the standard lowpass filter characteristic. The corresponding lowpass filter circuit is shown in Fig. 8.23(a).

If $C_1 = C_3 = C$ and $g_2 = g_4 = g_5 = g$, then it can be derived

$$g = \frac{2\omega_o C}{5Q}, \quad g_m = 5Q\omega_o C \left(1 - \frac{2}{25Q^2}\right), \quad K = 1 - \frac{2}{25Q^2} \tag{8.121}$$

The second interesting structure shown in Fig. 8.23(b) comes from the setting $Y_1 = g_1, Y_2 = g_2, Y_3 = sC_3, Y_4 = g_4, Y_5 = sC_5$. The transfer function is given by

$$H(s) = \frac{g_m g_2 g_4}{s^2 (g_1 + g_2) C_3 C_5 + s [(g_1 + g_2) g_4 C_3 + (g_1 g_2 + g_1 g_4 + g_2 g_4) C_5] + (g_1 + g_m) g_2 g_4} \tag{8.122}$$

This transfer function is very similar to the one in Eq. (8.120). So the lowpass filter in Fig. 8.23(b) will have similar performances as the one in Fig. 8.23(a).

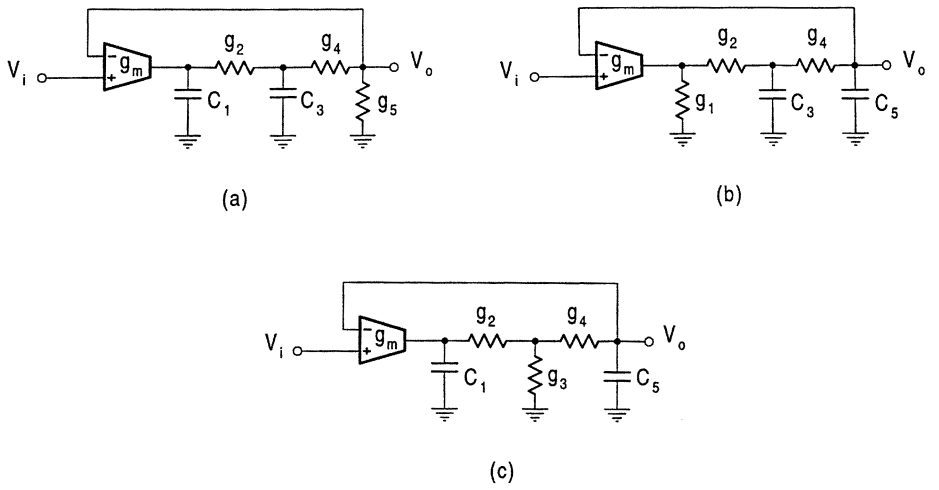

FIGURE 8.23
Three lowpass filters derived from Fig. 8.20.

The third lowpass filter is given in Fig. 8.23(c), which corresponds to $Y_1 = sC_1$, $Y_2 = g_2$, $Y_3 = g_3$, $Y_4 = g_4$, $Y_5 = sC_5$. The transfer function is derived as

$$H(s) = \frac{g_m g_2 g_4}{s^2 (g_2 + g_3 + g_4) C_1 C_5 + s [(g_2 + g_3) g_4 C_1 + g_2 (g_3 + g_4) C_5] + (g_m + g_3) g_2 g_4} \tag{8.123}$$

It can be shown that the lowpass structures in Fig. 8.23 all have low sensitivities. They contain two grounded capacitors and one grounded and two floating resistors and have similar performances for the nonidealities of the g_m OTA and the OTAs simulating the resistors, as will be seen in the next section.

8.7.4 Comments and Comparison

As discussed in Section 8.5, in integrated filter design, grounded capacitors are usually preferred because they have smaller parasitic capacitances and need less chip area than floating ones. The highpass filter contains two floating capacitors, bandpass filters use one grounded and one floating capacitors, and lowpass filters contain only grounded capacitors. Thus, the lowpass filters are better than the bandpass filters, which are better than the highpass filter in terms of the use of grounded capacitors.

In filter design the number of OTAs should be small, as more OTAs means larger chip area, larger power consumption, more noise, and more parasitic effects. As developed in Section 8.6, a grounded resistor needs one OTA to simulate, but a floating resistor requires two OTAs to simulate. Note also that the floating resistor when simulated using OTAs will introduce more equivalent parasitic elements (a π network, not an admittance). The highpass filter has three grounded resistors, bandpass filters have two grounded and one floating resistor, and lowpass filters embrace one grounded and two floating resistors. The numbers of OTAs needed for simulation of resistors in the highpass, bandpass, and lowpass filters are three, four, and five, respectively. Therefore, in terms of the number of OTAs the derived highpass structure is better than the bandpass filters, which are better than the lowpass filters.

The number of grounded capacitors and the number of grounded resistors are in conflict; if one is big, then the other must be small, as the total number is three. In real design some compromise may have to be made in order to achieve the global optimum.

The OTA is used as a differential input OTA in all highpass, bandpass, and lowpass structures. The nonideality effects of the g_m OTA will be similar for all the structures due to the similarity among the structures, although for example, in some structures such as Figs. 8.21, 8.22(a–c) and 8.23(b), the finite output conductance may be absorbed and in others such as Figs. 8.22(d), 8.23(a) and 8.23(c), the finite output capacitance may be absorbed. (A similar observation for the finite OTA input conductance and capacitance can also be discussed.)

The effects of nonidealities of the resistor simulation OTAs will be quite different. After absorption (see Section 8.6), the highpass filter in Fig. 8.21 will have three grounded parasitic capacitors in parallel with respective grounded resistors; the bandpass filters in Fig. 8.22 will have one floating and two grounded parasitic capacitors in parallel with the corresponding floating and grounded design resistors and one grounded parasitic resistor in parallel with the grounded capacitor; the lowpass filters in Fig. 8.23 will have two floating and one grounded parasitic capacitors in parallel with the related design resistors and two grounded parasitic resistors in parallel with respective design capacitors. It is thus clear that with respect to the effects of nonidealities of the OTAs simulating resistors, the highpass filter is the best, followed by the bandpass filters and then the lowpass filters. Again detailed analysis can be conducted by using the changed admittances due to the nonidealities of the resistor simulation OTAs to replace the ideal ones in Eq. (8.106) for any filter architectures.

8.8 Summary

In this chapter, we have used the operational transconductance amplifier to construct active filters. We have in particular presented systematic methods for generating second-order filters using a single OTA with a reasonable number of resistors and capacitors. The transfer functions, design formulas, and sensitivity results have been formulated. These OTA filters are insensitive to tolerance and parasitics, of high frequency capability, electronically tunable, and simple in structure. They are suitable for discrete implementation using commercially available OTAs and also useful for IC fabrication, when resistors are replaced by OTA equivalents, resulting in OTA-C filters. We have investigated OTA-C filters derived from the single OTA filters by resistor substitution. The effects of OTA nonidealities such as finite input and output impedances and transconductance frequency dependence have also been considered for both discrete and IC filters. It has been proved that these nonidealities influence filter performance. Some techniques have been suggested to reduce the effects from the structural standpoint.

It is noted that there are some other OTA filter structures. References [23] and [24] gave some single OTA structures with current input and voltage output. Filter architectures based on an OTA and an opamp were studied in Ref. [25]. The opamp may limit the working frequency, but in most cases it can be eliminated. OTA-C filters can also be obtained from single opamp active RC filters (as well as multiple opamp architectures) either by direct replacement of the opamp and resistors by OTAs or by some transformation [17]. Many more useful OTA-C filters will be introduced in the following chapters. In the next chapter we will investigate two integrator loop OTA-C filters. The current-mode equivalents of the single OTA filters developed in this chapter will be studied in Chapter 12.

References

[1] Mitra, S.K. and Hurth, C.F., Eds., *Miniatured and Integrated Filters*, John Wiley & Sons, New York, 1989.

[2] Laker, K.R. and Sansen, W., *Design of Analog Integrated Circuits and Systems*, McGraw-Hill, New York, 1994.

[3] Johns, D.A. and Martin, K., *Analog Integrated Circuit Design*, John Wiley & Sons, New York, 1997.

[4] Toumazou, C., Lidgey, F.J., and Haigh, D.G., Eds., *Analogue IC Design: the Current-Mode Approach*, Peter Peregrinus, London, 1990.

[5] Tsividis, Y.P. and Voorman, J.O., Eds., *Integrated Continuous-Time Filters: Principles, Design and Applications*, IEEE Press, 1993.

[6] Schaumann, R., Ghausi, M.S., and Laker, K.R., *Design of Analog Filters: Passive, Active RC and Switched Capacitor*, Prentice-Hall, NJ, 1990.

[7] Schaumann, R., Continuous-Time Integrated Filters, in *The Circuits and Filters Handbook*, Chen, W.K., Ed., CRC Press, Boca Raton, FL, 1995.

[8] Huelsman, L., *Active and Passive Analog Filter Design*, McGraw-Hill, New York, 1993.

[9] Wheatley, C.F. and Wittlinger, H.A., OTA obsoletes op. amp., *Proc. Nat. Electron. Conf.*, 152–157, 1969.

[10] Franco, S., Use transconductance amplifiers to make programmable active filters, *Electronic Design*, 98–101, Sep. 1976.

[11] Malvar, H.S., Electronically tunable active filters with operational transconductance amplifiers, *IEEE Trans. Circuits Syst.*, 29(5), 333–336, 1982.

[12] Bialko, M. and Newcomb, R.W., Generation of all finite linear circuits using the integrated DVCCS, *IEEE Trans. Circuit Theory*, 18, 733–736, 1971.

[13] Urbaś, A. and Osiowski, J., High-frequency realization of C-OTA second order active filters, *Proc. IEEE Intl. Symp. Circuits Syst.*, 1106–1109, 1982.

[14] Malvar, H.S., Electronically controlled active-C filters and equalizers with operational transconductance amplifiers, *IEEE Trans. Circuits Syst.*, 31(7), 645–649, 1984.

[15] Geiger, R.L. and Sánchez-Sinencio, E., Active filter design using operational transconductance amplifiers: a tutorial, *IEEE Circuits and Devices Magazine*, 20–32, Mar. 1985.

[16] Sánchez-Sinencio, E., Geiger, R.L., and Nevarez-Lozano, H., Generation of continuous-time two integrator loop OTA filter structures, *IEEE Trans. Circuits Syst.*, 35(8), 936–946, 1988.

[17] Ananda Mohan, P.V., Generation of OTA-C filter structures from active RC filter structures, *IEEE Trans. Circuits Syst.*, 37, 656–660, 1990.

[18] Acar, C., Anday, F., and Kuntman, H., On the realization of OTA-C filters, *Intl. J. Circuit Theory Applications*, 21(4), 331–341, 1993.

[19] Sun, Y. and Fidler, J.K., Novel OTA-C realizations of biquadratic transfer functions, *Intl. J. Electronics*, 75, 333–348, 1993.

[20] Sun, Y. and Fidler, J.K., Resonator-based universal OTA-grounded capacitor filters, *Intl. J. Circuit Theory Applications*, 23, 261–265, 1995.

[21] Tan, M.A. and Schaumann, R., Design of a general biquadratic filter section with only transconductance and grounded capacitors, *IEEE Trans. Circuits Syst.*, 35(4), 478–480, 1988.

[22] Nawrocki, R. and Klein, U., New OTA-capacitor realization of a universal biquad, *Electron. Lett.*, 22(1), 50–51, 1986.

[23] Al-Hashimi, B.M. and Fidler, J.K., Novel high-frequency continuous-time low-pass OTA based filters, *Proc. IEEE Intl. Symp. Circuits Syst.*, 1171–1172, 1990.

[24] Al-Hashimi, B.M., Fidler, J.K., and Garner, P., High frequency active filters using OTAs, *Proc. IEE Colloquium on Electronic Filters*, 3/1–3/5, London, 1989.

[25] Deliyannis, T., Active RC filters using an operational transconductance amplifier and an operational amplifier, *Intl. J. Circuit Theory Applications*, 8, 39–54, 1980.

[26] Sun, Y., Jefferies, B., and Teng, J., Universal third-order OTA-C filters, *Intl. J. Electronics*, 80, 1998.

[27] Nawrocki, R., Building set for tunable component simulation filters with operational transconductance amplifiers, *Proc. Midwest Symp. Circuits and Systems*, 227–230, 1987.

[28] Tan, M.A. and Schaumann, R., Simulating general-parameter filters for monolithic realization with only transconductance elements and grounded capacitors, *IEEE Trans. Circuits Syst.*, 36(2), 299–307, 1989.

[29] de Queiroz, A.C.M., Caloba, L.P., and Sánchez-Sinencio, E., Signal flow graph OTA-C integrated filters, *Proc. IEEE Intl. Symp. Circuits Syst.*, 2165–2168, 1988.

[30] Nawrocki, R., Electronically tunable all-pole low-pass leapfrog ladder filter with operational transconductance amplifier, *Intl. J. Electronics*, 62(5), 667–672, 1987.

[31] Sun, Y. and Fidler, J.K., Synthesis and performance analysis of a universal minimum component integrator-based IFLF OTA-grounded capacitor filter, *IEE Proceedings: Circuits, Devices and Systems*, 143, 107–114, 1996.

[32] Sun, Y. and Fidler, J.K., Structure generation and design of multiple loop feedback OTA-grounded capacitor filters, *IEEE Trans. on Circuits and Systems, Part-I: Fundamental Theory and Applications*, 44(1), 1–11, 1997.

[33] Nawrocki, R., Electronically controlled OTA-C filter with follow-the-leader-feedback structures, *Intl. J. Circuit Theory Applications*, 16, 93–96, 1988.

[34] Nevarez-Lozano, H., Hill, J.A., and Sánchez-Sinencio, E., Frequency limitations of continuous-time OTA-C filters, *Proc. IEEE Intl. Symp. Circuits Syst.*, 2169–2172, 1988.

[35] Sun, Y. and Fidler, J.K., Performance analysis of multiple loop feedback OTA-C filters, *Proc. IEE 14th Saraga Colloquium on Digital and Analogue Filters and Filtering Systems*, 9/1–9/7, London, 1994.

[36] Ramírez-Angulo, J. and Sánchez-Sinencio, E., Comparison of biquadratic OTA-C filters from the tuning point of view, *Proc. IEEE Midwest Symp. Circuits Syst.*, 510–514, 1988.

[37] Park, C.S. and Schaumann, R., Design of a 4-MHz analog integrated CMOS transconductance-C bandpass filter, *IEEE J. Solid-State Circuits*, 23(4), 987–996, 1988.

[38] Silva-Martinez, J., Steyaert, M.S.J., and Sansen, W., A 10.7-MHz 68-dB SNR CMOS continuous-time filter with on-chip automatic tuning, *IEEE J. Solid-State Circuits*, 27, 1843–1853, 1992.

[39] Loh, K.H., Hiser, D.L., Adams, W.J., and Geiger, R.L., A versatile digitally controlled continuous-time filter structure with wide range and fine resolution capability, *IEEE Trans. Circuits Syst.*, 39, 265–276, 1992.

[40] Nedungadi, A.P. and Geiger, R.L., High-frequency voltage-controlled continuous-time low-pass filter using linearized CMOS integrators, *Electron. Lett.*, 22, 729–731, 1986.

[41] Gopinathan, V., Tsividis, Y.P., Tan, K.S., and Hester, R.K., Design considerations for high-frequency continuous-time filters and implementation of an antialiasing filter for digital video, *IEEE J. Solid-State Circuits*, 25(6), 1368–1378, 1990.

[42] Wang, Y.T. and Abidi, A.A., CMOS active filter design at very high frequencies, *IEEE J. Solid-State Circuits*, 25(6), 1562–1574, 1990.

[43] Sun, Y. and Fidler, J.K., Structure generation of current-mode two integrator loop dual output-OTA grounded capacitor filters, *IEEE Trans. on Circuits and Systems, Part II: Analog and Digital Signal Proc.*, 43(4), 1996.

[44] Fidler, J.K., Mack, R.J., and Noakes, P.D., Active filters incorporating the voltage-to-current transactor, *Microelectronics J.*, 8, 19–22, 1977.

[45] Al-Hashimi, B.M. and Fidler, J.K., A novel VCT-based active filter configuration, *Proc. 6th Intl. Symp. Networks, Systems and Signal Proc.*, Yugoslavia, Jun. 1989.

[46] Fidler, J.K., Sensitivity assessment of parasitic effects in second-order active-filter configurations, *Electronic Circuits and Systems*, 2(6) 181–185, 1978.

[47] Weyton, L., A useful sensitivity measure for second order RC active filter configuration, *IEEE Trans. Circuits and Syst.*, 23, 506–508, 1976.

[48] Sallen, R.P. and Key, E.L., A practical method of designing RC active filters, *IRE Trans. Circuit Theory*, 2, 74–85, 1955.